

# Resource Allocation in Virtualized CoMP-NOMA HetNets: Multi-Connectivity for Joint Transmission

Sepehr Rezvani, Nader Mokari, *Senior Member, IEEE*, Mohammad R. Javan,  
*Senior Member, IEEE*, and Eduard A. Jorswieck, *Fellow, IEEE*

## Abstract

In this work, we design a generalized joint transmission coordinated multi-point (JT-CoMP)-non-orthogonal multiple access (NOMA) model for a virtualized multi-infrastructure network. In this model, all users benefit from multiple joint transmissions of CoMP thanks to the multi-connectivity opportunity provided by wireless network virtualization (WNV) in multi-infrastructure networks. The NOMA protocol in CoMP results in an unlimited NOMA clustering (UNC) scheme, where the order of each NOMA cluster is the maximum possible value. We show that UNC results in maximum successful interference cancellation (SIC) complexity at users. In this regard, we propose a limited NOMA clustering (LNC) scheme, where the SIC is performed to only a subset of users. We formulate the problem of joint power allocation and user association for the UNC and LNC schemes. Then, one globally and one locally optimal solution are proposed for each problem based on mixed-integer monotonic optimization and

S. Rezvani and E. A. Jorswieck are with the Department of Information Theory and Communication Systems, Technische Universität Braunschweig, Braunschweig, Germany (e-mails: {rezvani,jorswieck}@ifn.ing.tu-bs.de).

N. Mokari is with the Department of Electrical and Computer Engineering, Tarbiat Modares University, Tehran, Iran.

M. R. Javan is with the Department of Electrical and Robotics Engineering, Shahrood University of Technology, Shahrood, Iran.

sequential programming, respectively. Numerical assessments reveal that WNV and LNC improves users sum-rate and reduces users SIC complexity by up to 35% and 46% compared to the non-virtualized CoMP-NOMA system and UNC model, respectively. Therefore, the proposed algorithms are suitable candidates for the implementation on open and intelligent radio access networks.

### Index Terms

Coordinated multi-point, NOMA, wireless network virtualization, global programming, monotonic optimization, sequential programming, convex optimization.

## I. INTRODUCTION

Among various existing coordinated multi-point (CoMP) techniques for mitigating inter-cell interference (ICI) in multi-cell wireless networks, joint transmission CoMP (JT-CoMP) has attracted significant attention. In JT-CoMP, multiple base stations (BSs) are allowed to schedule/transmit the same message to a user over the same frequency band which facilitates ICI management and empowers the received signals at users<sup>1</sup> [1]–[3]. By introducing the orthogonal multiple access (OMA) techniques on CoMP, the overall interference caused by coordinated BSs (CoMP-BSs) will be eliminated at the CoMP-user. However, OMA restricts the coordination opportunities in CoMP [4], [5]. To overcome this issue, power-domain non-orthogonal multiple access (NOMA)<sup>2</sup> is introduced on CoMP, called CoMP-NOMA, where the resource blocks are shared between users under the successive interference cancellation (SIC) technique which improves both the spectral efficiencies and users connectivity [2]–[6].

In multi-infrastructure wireless networks operating in different protected frequency bands, each user is restricted to subscribe to only one infrastructure provider (InP) [7], [8]. This restriction

<sup>1</sup>In this work, the term CoMP is referred to JT-CoMP.

<sup>2</sup>In this work, the term NOMA is referred to power-domain NOMA.

degrades the users connectivity, specifically for the cell-center users who are close to the co-located BSs belonging to different InPs. There has been numerous studies to design efficient methods for sharing InPs resources by means of wireless network virtualization (WNV) [7]–[9]. In WNV, InPs lease their scheduled resources to a number of virtual networks, also called mobile virtual network operators (MVNOs). Each MVNO acts as a service provider for its subscribed users based on the service level agreements (SLAs) between MVNOs and end-users [7]–[10]. In virtualized multi-infrastructure networks, co-located BSs of different InPs form a virtual BS (VBS). Hence, users with strict SLA can be connected to the nearby VBS to benefit from the multi-connectivity opportunity<sup>3</sup> provided by WNV improving the spectral and energy efficiencies [9]. Accordingly, WNV can be introduced on multi-infrastructure CoMP-NOMA systems, where cell-center users can be connected to the nearby VBS saving more physical resources for the cell-edge users. Besides, nearby VBSs can jointly transmit/schedule signals to the cell-edge users, specifically ICI-prone users suffering from poor channel qualities providing better user fairness and massive connectivity. However, virtualized CoMP-NOMA needs a centralized resource management to fully utilize the benefits of WNV on multi-infrastructure CoMP-NOMA and fulfill global constraints, e.g., user scheduling, which may be impractical due to the isolated resource management between InPs. Software-defined networking (SDN) is the promising solution for this issue enabling separation of the control plane from the data plane. Furthermore, SDN enables the centralized controlling by means of connected switches and routers to all the network elements which improves the network flexibility and scalability [9]. Despite the huge potential of software-defined virtualized CoMP-NOMA (SV-CoMP-NOMA), resource management is not straightforward in this system, due to the following challenges:

- 1) ***SIC Ordering***: In CoMP, multiple copies of a message is transmitted from CoMP-BSs to

<sup>3</sup>The term 'multi-connectivity', also called inter-frequency multi-connectivity, refers to the association of a user to multiple InPs over orthogonal bands by applying WNV.

each CoMP-user with arbitrary power allocation. Hence, the CoMP system with arbitrary power allocation is identical to the multiple-input single-output (MISO) Gaussian broadcast channel (BC) with per-antenna power constraint (PAPC) [11]. Due to the nondegradation of MISO Gaussian BCs with PAPC [11], [12], the capacity region of CoMP can be achieved by linear preprocessing combined with dirty paper coding (DPC) proposed in [13]. Therefore, in contrast to the single-input single-output (SISO) Gaussian BCs which are degraded [14], [15], NOMA in CoMP (with arbitrary power allocation) is not capacity achieving<sup>4</sup>. One direct result of nondegraded CoMP systems is that the optimal SIC ordering in single-cell NOMA which follows the ascending order of NOMA users' channel gain normalized by noise is not optimal in CoMP-NOMA [2], [16]. In general, the optimal SIC ordering in CoMP-NOMA depends not only on the channel gains and noise, but also on the power allocation strategy.

- 2) ***Joint Power Allocation, CoMP Scheduling, and NOMA Clustering:*** The joint transmission CoMP is proposed as an efficient, yet suboptimal [17], strategy to improve the achievable rates in the interference networks, specifically for high-demand cell-edge users suffering from strong interferences [13]. Recently, it is shown that adopting CoMP transmission to only cell-edge users may not be beneficial for the system [18], [19]. Actually, cell-edge users with low SLAs do not need to be scheduled in CoMP transmission while some cell-center users with strict SLA may need CoMP transmissions. In NOMA, it is verified that the power allocation is a key factor to maximize the achievable spectral efficiency [20]–[22]. Moreover, the traditional power allocation for spectral efficiency maximization in multi-cell NOMA systems may not be efficient for other cells calling the design of a

<sup>4</sup>The main advantage of NOMA compared to DPC is its low complexity interference cancellation structure, although it is not capacity achieving in CoMP. The performance gap between NOMA and DPC depends on the diversity order of channel gains which can be considered as a future work.

generalized CoMP-NOMA model with efficient joint power allocation, CoMP scheduling, i.e., determining the set of CoMP-users and their coordinated BSs (CoMP-BSs), and NOMA clustering.

- 3) ***SIC Complexity at CoMP-users:*** According to the NOMA protocol, at each user pair connected to the same BS over the same frequency band, one user (with higher decoding order) should fully decode and cancel the signal of other user [23], [24]. In CoMP-NOMA, each CoMP-user belongs to multiple cells NOMA clusters<sup>5</sup> depending on the number of CoMP-BSs. As a result, the order of NOMA clusters of CoMP-NOMA is typically larger than in traditional multi-cell NOMA systems [2], [3]. The traditional approach which limits the number of multiplexed users over the shared frequency band in each cell [20], [25] has no refined control on the increased order of NOMA clusters due to the joint transmission of CoMP. This requires a design of a low-complexity NOMA clustering scheme, where each CoMP-user performs SIC to only a subset of potential users in its NOMA cluster.

Resource allocation in CoMP-NOMA consists of three parts: CoMP scheduling which determines the set of CoMP and non-CoMP users with their CoMP-BSs, NOMA clustering of all users, and centralized power allocation. An opportunistic NOMA clustering scheme for a group of CoMP-users at cell-edge is designed in [5] by adopting an efficient power allocation algorithm. A novel multi-tier NOMA scheme is proposed in [4] to serve CoMP-users with poor channel qualities by relaying signals to them. A selective-transmission strategy for determining the set of CoMP-BSs for a fixed power allocation strategy in CoMP-NOMA is proposed in [26]. The authors in [3] first design a CoMP-NOMA model, where CoMP scheduling and NOMA clustering are heuristically determined. Then, two centralized and distributed power allocation algorithms per-NOMA cluster are proposed to maximize users spectral efficiency in the NOMA cluster. In the mentioned works, the joint transmission of CoMP is considered for only cell-edge

<sup>5</sup>The NOMA cluster of each cell is called local NOMA set.

users. For instance, in [3], the set of CoMP-users are determined based on the received signal strength (RSS) at users. And, users with weak RSS, i.e., cell-edge users, are scheduled for joint transmission. A number of research efforts addressed the benefits of joint transmission of CoMP-NOMA for both the cell-edge and cell-center users in improving overall spectral efficiency [18], [27], and lowering outage probability [19]. In [18], the CoMP scheduling and NOMA clustering are heuristically determined based on the quality of service (QoS) requirements of users. Then, a locally optimal joint beamforming and power allocation is designed. The fundamentals of mutual SIC in CoMP-NOMA for 2-user and 3-user systems are investigated in [27], where the users simultaneously cancel their corresponding interfering signals. In [19], a generalized CoMP-NOMA system is proposed, where all the users are considered as potential CoMP-users. It is shown that generalizing CoMP to all the users improves the overall spectral efficiency. However, generalized CoMP-NOMA inherently increases the NOMA clustering orders when the number of CoMP-BSs grows. To reduce the order of NOMA clusters, a heuristic low-complexity<sup>6</sup> NOMA clustering strategy based on the channel qualities is devised, where the order of CoMP-BSs is reduced. After defining the NOMA clusters, an optimal power allocation strategy per NOMA cluster is proposed. Since CoMP scheduling and NOMA clustering affect the interference level at users, the joint power allocation, CoMP scheduling, and NOMA clustering would result in the maximum overall spectral efficiency [3]. However, the combinatorial nature of user scheduling complicates the joint strategy [3]. Addressing these strategies jointly is still an open problem. Besides, the power allocation strategies in [3], [19] are devised for each NOMA cluster independently. These strategies may not be efficient for the users forming multiple NOMA clusters since for such users, the allocated powers through all the NOMA clusters should be optimized jointly. Also, all the prior studies on CoMP-NOMA considered a single InP. Therefore,

<sup>6</sup>In this context, the term complexity is referred to the complexity of SIC which is directly proportional to the order of NOMA clusters, i.e., the number of multiplexed users within a NOMA cluster.

the impact of isolation among co-located BSs, and applications of WNV in providing the multi-connectivity opportunity for CoMP-NOMA are not yet addressed.

In the current study, we consider a multi-infrastructure heterogeneous network (HetNet) consisting of multiple isolated InPs and apply our proposed SV-CoMP-NOMA system to this network. The main contributions are summarized as follows:

- We propose a generalized CoMP-NOMA model, where both the cell-edge and cell-center users are considered as potential CoMP-users, and the set of CoMP-BSs (CoMP-set) of each CoMP-user could be partially or completely different to the CoMP-set of other CoMP-users.
- We analyze the NOMA protocol in the generalized CoMP-NOMA system, called CoMP-NOMA protocol. This protocol results in the unlimited NOMA clustering (UNC) model, where each CoMP-user forms a global NOMA set consisting of all the users connected to at least one of its CoMP-BSs on the assigned wireless bandwidth. We show that UNC inherently increases the order of NOMA clusters, and subsequently the SIC complexity at users.
- A low-complexity NOMA clustering scheme, called limited NOMA clustering (LNC), is designed to reduce the order of NOMA clusters for performing SIC. In this scheme, the SIC of NOMA is performed to a subset of users within the global NOMA set.
- We formulate the joint power allocation and user association problems in the UNC and LNC models to maximize users sum-rate subject to their QoS requirements. In these problems, CoMP scheduling and NOMA clustering are determined by the user association indicator.
- The optimization problems are nonconvex and NP-hard. To solve each problem, we propose one globally and one locally optimal solution. The globally optimal solution is based on mixed-integer monotonic optimization. The locally optimal solution is based on the successive convex approximation (SCA) algorithm. To apply these methods, we first perform a series of transformations to make the problems tractable.
- Numerical results show that the joint optimization of power allocation, CoMP scheduling,

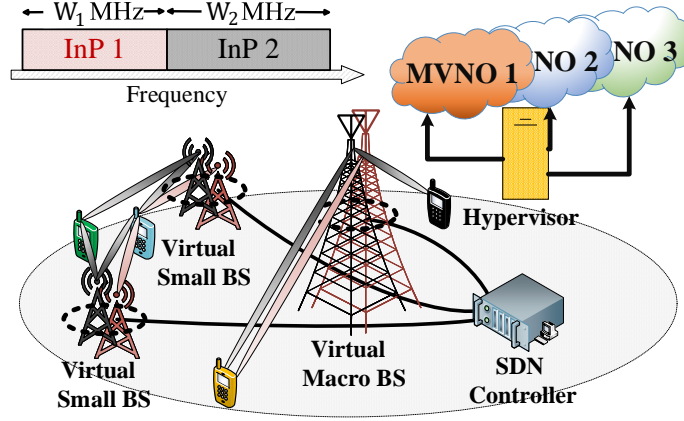


Fig. 1. Exemplary illustration of the SV-CoMP-NOMA system in a 2-infrastructure HetNet, where each user can be associated to multiple nearby VBSs on orthogonal bands.

and NOMA clustering outperforms the existing power allocation algorithms by up to 17%. Moreover, LNC reduces the SIC complexity of users in UNC by up to 46%. Furthermore, applying WNV to CoMP-NOMA systems, and CoMP to virtualized NOMA systems result in performance gains of nearly 35% and 20%, respectively.

The rest of this paper is organized as follows: Section II describes the SV-CoMP-NOMA system, and NOMA clustering and SIC ordering models, and then formulates the UNC and LNC optimization problems. These problems are solved in Section III. Section IV provides the simulation results. Finally, our conclusions are presented in Section V.

## II. SYSTEM MODEL

### A. Network Model

We consider the downlink transmission of a multi-user multi-infrastructure HetNet as shown in Fig. 1. This network consists of multiple InPs each of which includes a specific set of single-antenna BSs, and a dedicated licensed wireless band ( $W_i$  Hz for InP  $i$ ) that is orthogonal to other InPs [8]. The set of InPs and the set of BSs owned by InP  $i$  are denoted by  $\mathcal{I} = \{1, \dots, I\}$



and  $\mathcal{B}_i = \{0, \dots, B_i\}$ , respectively. The set of  $K$  single-antenna users is indicated by  $\mathcal{K} = \{1, \dots, K\}$ . Moreover, a hypervisor located on the top of InPs is responsible for collecting users information and virtualizing InPs resources [10]. In addition, a SDN controller with a global view of the network<sup>7</sup> is responsible for the centralized resource management [9]. We assume that the perfect channel state information (CSI) of all users is available at each BS obtained based on the channel estimation approaches studied in the literature<sup>8</sup> [18], [28], [29].

In this network, there are  $V$  MVNOs with the set of  $\mathcal{V} = \{1, \dots, V\}$ . Each MVNO  $v$  acts as a service provider for its subscribed users in  $\mathcal{K}_v$ . Moreover, each user is owned by only one MVNO, i.e.,  $\bigcup_{v \in \mathcal{V}} \mathcal{K}_v \triangleq \mathcal{K}$  and  $\mathcal{K}_v \cap \mathcal{K}_{v'} \triangleq \emptyset, \forall v, v' \in \mathcal{V}, v' \neq v$  [30]. To reduce conflicts between MVNOs, a specific minimum data rate  $R_v^{\text{rsv}}$  is contracted between each MVNO  $v$  and users in  $\mathcal{K}_v$  [30], [31]. In this system, WNV breaks the isolation among InPs. In fact, each MVNO can lease the physical and radio resources of multiple InPs. In this way, WNV provides the multi-connectivity opportunity over orthogonal bandwidths. The term "multi-connectivity" refers to the inter-frequency multi-connectivity of users. As a result, each user can be associated to the BSs owned by different InPs. Similar to the multi-carrier technology, it is assumed that each user receives a specific message over each orthogonal bandwidth. Let us denote the user association indicator by  $\theta_{i,b,k} \in \{0, 1\}$ , where  $\theta_{i,b,k} = 1$  if user  $k$  is associated to the  $b^{\text{th}}$  BS of InP  $i$  (on bandwidth  $W_i$ ), and otherwise,  $\theta_{i,b,k} = 0$ . Due to the isolation among InPs, when WNV is not applied, each user can be assigned to only one InP. In other words, for the case that WNV is not applied, the scheduler should guarantee the following isolation constraint as

$$\theta_{i,b,k} + \theta_{i',b',k} \leq 1, \forall k \in \mathcal{K}, i, i' \in \mathcal{I}, i' \neq i, b \in \mathcal{B}_i, b' \in \mathcal{B}_{i'}. \quad (1)$$

<sup>7</sup>The central SDN controller has all the users and InPs information, like CSI, SLAs, network topology and configuration, and etc. This controller can be located anywhere in the network.

<sup>8</sup>Similar to the related works on CoMP-NOMA e.g., [2]–[4], [6], [18], we assume that the CSI is perfectly available at the SDN controller. In this work, we aim to illustrate the maximum gain achieved with the joint power allocation, NOMA clustering, and CoMP scheduling strategy. The impact of imperfect CSI is considered as our future work.

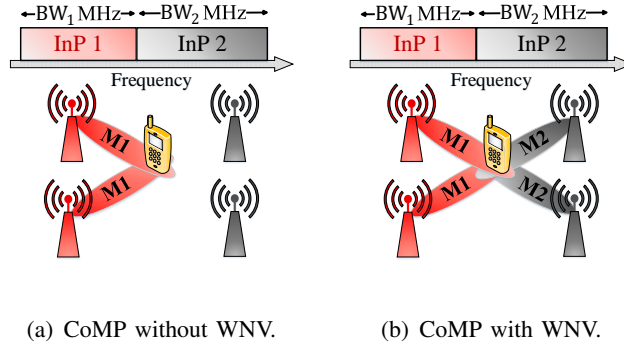


Fig. 2. A two-infrastructure CoMP system with/without WNV. In these figures, it is assumed that messages M1 and M2 are sent by the CoMP-BSs of InPs 1 and 2, respectively.

Besides, we consider a more flexible scheme, where MVNOs can operate in the same bandwidth. This scheme refers to breaking the isolation among MVNOs, where users subscribed to different MVNOs can receive signals over the same bandwidth. The superiority of breaking the isolation among MVNOs is to provide a more flexible NOMA clustering among users. In this case, regardless of the association of users to MVNOs, the users with the highest channel gain differences can form a NOMA cluster [31]. Assume that the joint transmission of CoMP is applied to the virtualized multi-infrastructure system. The users connectivity under the joint transmission of CoMP refers to the intra-frequency dual-connectivity, where CoMP-BSs transmit the same message (multiple copies of a message) to a CoMP-user. An exemplary illustration of the virtualized CoMP system and its comparison to a non-virtualized CoMP system (with isolation among InPs) is shown in Fig. 2. Fig. 2(a) shows a non-virtualized CoMP system in which the reference user is assigned to only InP 1 operating in bandwidth  $W_1$ . This user receives message M1 from its CoMP-BSs owned by InP 1 (BSs with red color). Fig. 2(b) shows a virtualized CoMP system, where the reference user receives message M1 from its CoMP-BSs of InP 1 and message M2 from its CoMP-BSs of InP 2.

### B. SV-CoMP-NOMA System

Here, we apply NOMA (with SIC) to the virtualized CoMP system resulting in virtualized CoMP-NOMA system. In the generalized CoMP-NOMA model, the CoMP-set of each CoMP-user could be partially or completely different to other CoMP-users. According to the NOMA protocol, if two users receive signals from the same transmitter (simultaneously over the same frequency band), these users form a NOMA cluster in which one user (with higher decoding order) is enforced to fully decode and cancel the signal of other user, while the signal of the user with higher decoding order is treated as noise (called intra-NOMA interference (INI)). The SIC of NOMA implies that each user should fully decode and cancel the signals of other users within the same NOMA cluster (associated to the same transmitter) with lower decoding orders. The signals of other users that do not belong to this NOMA cluster (associated to other transmitters) are fully treated as noise (called ICI). According to the CoMP protocol, each user first receives coherent superpositions of its desired signal from its CoMP-BSs. Then, it decodes the whole received signal [2], [3], [32]. When NOMA is introduced on CoMP, the CoMP-NOMA protocol can be described as follows: If the intersection of the CoMP-set of two CoMP-users is non-empty, these users belong to the same NOMA cluster. In each user pair within the NOMA cluster, one user should fully decode and cancel the signal(s) (superposition of the desired signal) of other user depending on the decoding order. For example, assume that BS 1 belongs to the CoMP-set of CoMP-users 1 and 2. The NOMA protocol at BS 1 enforces users 1 and 2 to form a NOMA cluster. According to the CoMP protocol, if user 1 has a higher decoding order, this user is enforced to fully decode and cancel the signals of CoMP-user 2. The NOMA clustering under the CoMP-NOMA protocol is presented in the following subsection.

1) *Unlimited NOMA Clustering*: In the generalized CoMP-NOMA model, the CoMP-set of user  $k$  in bandwidth  $W_i$  is denoted by  $\mathcal{C}_{i,k} = \{b \in \mathcal{B}_i \mid \theta_{i,b,k} = 1\}$ . For the case that user  $k$  is connected to only one BS over bandwidth  $W_i$ , i.e.,  $|\mathcal{C}_{i,k}| = 1$  or  $\sum_{b_i \in \mathcal{B}_i} \theta_{i,b,k} = 1$ , the user is

referred to "non-CoMP-user". The NOMA clustering protocol among the non-CoMP-users is the same as the NOMA protocol of the traditional multi-cell NOMA systems [3], [33], [34]. According to the CoMP-NOMA protocol, if  $\mathcal{C}_{i,k} \cap \mathcal{C}_{i,k'} \neq \emptyset$  or equivalently  $\sum_{b \in \mathcal{B}_i} \theta_{i,b,k} \theta_{i,b,k'} \geq 1$ , users  $k$  and  $k'$  belong to the same NOMA cluster on bandwidth  $W_i$ , meaning that one user should fully decode and cancel the signal(s) of other user depending on the decoding order on bandwidth  $W_i$ . Assume that  $\lambda_{i,k} \in \{1, 2, \dots, K\}$  is the SIC decoding order indicator of user  $k$  on bandwidth  $W_i$ , and  $\lambda_{i,k} > \lambda_{i,k'}$  indicates that user  $k$  has a higher decoding order than user  $k'$  on bandwidth  $W_i$ . The set of decoded and canceled users in cell  $b$  by user  $k$  on bandwidth  $W_i$  can be obtained by  $\Phi_{i,b,k}^{\text{Cell}} = \{k' \in \mathcal{K} \mid \theta_{i,b,k} \theta_{i,b,k'} = 1, \lambda_{i,k} > \lambda_{i,k'}\}$ . According to the CoMP-NOMA protocol, the set of decoded and canceled users by user  $k$  on bandwidth  $W_i$  is  $\Phi_{i,k} = \cup_{b \in \mathcal{B}_i} \Phi_{i,b,k}^{\text{Cell}} = \{k' \in \mathcal{K} \mid \sum_{b \in \mathcal{B}_i} \theta_{i,b,k} \theta_{i,b,k'} \geq 1, \lambda_{i,k} > \lambda_{i,k'}\}$ . The set  $\Phi_{i,k}$  is called the global set of users decoded and canceled by user  $k$  on bandwidth  $W_i$  (or in summary the global NOMA set of user  $k$  on bandwidth  $W_i$ ). The set  $\Phi_{i,b,k}^{\text{Cell}}$  is called the local set of users decoded and canceled by user  $k$  on bandwidth  $W_i$  (or in summary the local NOMA set of user  $k$  on bandwidth  $W_i$ ). In UNC, the SIC is performed according to the global NOMA set of users indicated by  $\Phi_{i,k}$ . Note that the decoding order  $\lambda_{i,k} > \lambda_{i,k'}$  for the user pair  $(k, k')$  belonging to the same NOMA cluster over bandwidth  $W_i$  means that at each cell in  $\mathcal{C}_{i,k} \cap \mathcal{C}_{i,k'}$ , the SIC decoding order follows  $\lambda_{i,k} > \lambda_{i,k'}$ . The superposition coding at the BSs in  $\mathcal{C}_{i,k} \cap \mathcal{C}_{i,k'}$  also follows the decoding order  $\lambda_{i,k} > \lambda_{i,k'}$ . In other words, the SIC decoding order among each user pair belonging to the same NOMA cluster is the same at all the associated cells (so the local NOMA sets) [2], [3]. Besides, the signal(s) of user  $k'$  is treated as INI at user  $k$  if users  $k$  and  $k'$  belong to the same NOMA cluster, i.e.,  $\sum_{b \in \mathcal{B}_i} \theta_{i,b,k} \theta_{i,b,k'} \geq 1$ , and user  $k'$  has a higher decoding order than user  $k$ , i.e.,  $\lambda_{i,k'} > \lambda_{i,k}$ . The set of interfering NOMA users (resulting in INI) at user  $k$  on bandwidth  $W_i$  is indicated by  $\Phi_{i,k}^{\text{INI}} = \left\{ k' \in \mathcal{K} \mid \min \left\{ \sum_{b \in \mathcal{B}_i} \theta_{i,b,k} \theta_{i,b,k'}, 1 \right\} = 1, \lambda_{i,k'} > \lambda_{i,k} \right\}$ . The signal(s) of user  $k'$  is treated as ICI at user  $k$  if users  $k$  and  $k'$  do not belong to the same

NOMA cluster, i.e.,  $\sum_{b \in \mathcal{B}_i} \theta_{i,b,k} \theta_{i,b,k'} = 0$ . The set of users whose signal(s) are considered as ICI at user  $k$  is denoted by  $\Phi_{i,k}^{\text{ICI}} = \{k' \in \mathcal{K} \mid \sum_{b \in \mathcal{B}_i} \theta_{i,b,k} \theta_{i,b,k'} = 0\}$ . We call this set as the ICI set of user  $k$  on bandwidth  $W_i$ . Similar to the definition of ICI in traditional multi-cell NOMA, the signal(s) of users belonging to the ICI set of a user will not be decoded and canceled by that user at all, so are fully treated as AWGN. In UNC, the CoMP-user does not experience any ICI by its CoMP-BSs over the assigned bandwidth. However, the CoMP-user may do experience INI incurred by its CoMP-BSs depending on the SIC decoding order. Besides, each CoMP-user has multiple local NOMA sets depending on the order of its CoMP-set [3]. Accordingly, each local NOMA set of the CoMP-user is a subset of its global NOMA set. The non-CoMP-user (which is associated to only one BS) has only one local NOMA set. As a result, the local NOMA set of each non-CoMP-user is equivalent to its global NOMA set.

In this work, we assume that the BSs employ maximum ratio transmission (MRT) under instantaneous CSI [2], [3], [6], [18], [35]. Let  $d_{i,k} \sim \mathcal{CN}(0, 1)$  be the desired signal of user  $k$  scheduled to be transmitted on bandwidth  $W_i$  [18]. The channel gain from BS  $b \in \mathcal{B}_i$  to user  $k$  is denoted by  $g_{i,b,k}$ . Moreover, the transmit power of BS  $b \in \mathcal{B}_i$  to user  $k$  is indicated by  $p_{i,b,k}$ . After successful SIC at users, the received signal at user  $k$  on bandwidth  $W_i$  is given by

$$y_{i,k} = \underbrace{\sum_{b \in \mathcal{C}_{i,k}} \sqrt{p_{i,b,k}} g_{i,b,k} d_{i,k}}_{\text{desired signal}} + \underbrace{\sum_{k' \in \Phi_{i,k}^{\text{INI}}} \sum_{b \in \mathcal{C}_{i,k'}} \sqrt{p_{i,b,k'}} g_{i,b,k} d_{i,k'}}_{\text{INI}} + \underbrace{\sum_{k' \in \Phi_{i,k}^{\text{ICI}}} \sum_{b \in \mathcal{C}_{i,k'}} \sqrt{p_{i,b,k'}} g_{i,b,k} d_{i,k'}}_{\text{ICI}} + N_{i,k}, \quad (2)$$

where the first term is the received desired signal at user  $k$ , and the second and third terms are the INI and ICI at user  $k$ , respectively. The term  $N_{i,k}$  is the additive white Gaussian noise (AWGN) at user  $k$  on bandwidth  $W_i$  with zero mean and variance  $\sigma_{i,k}^2$ . The received signal of user  $k$  on bandwidth  $W_i$  can be reformulated as

$$y_{i,k} = \underbrace{\sum_{b \in \mathcal{B}_i} \theta_{i,b,k} \sqrt{p_{i,b,k}} g_{i,b,k} d_{i,k}}_{\text{desired signal}} + \underbrace{\sum_{\substack{k' \in \mathcal{K}, \\ \lambda_{i,k'} > \lambda_{i,k}}} \min \left\{ \sum_{b \in \mathcal{B}_i} \theta_{i,b,k} \theta_{i,b,k'}, 1 \right\} \sum_{b \in \mathcal{B}_i} \theta_{i,b,k'} \sqrt{p_{i,b,k'}} g_{i,b,k} d_{i,k'}}_{\text{INI}}$$

$$+ \underbrace{\sum_{\substack{k' \in \mathcal{K}, \\ k' \neq k}} \left( 1 - \min \left\{ \sum_{b \in \mathcal{B}_i} \theta_{i,b,k} \theta_{i,b,k'}, 1 \right\} \right) \sum_{b \in \mathcal{B}_i} \theta_{i,b,k'} \sqrt{p_{i,b,k'}} g_{i,b,k} d_{i,k'}}_{\text{ICI}} + N_{i,k}. \quad (3)$$

In (3), the term  $\min \left\{ \sum_{b \in \mathcal{B}_i} \theta_{i,b,k} \theta_{i,b,k'}, 1 \right\}$  is the NOMA clustering indicator which can take 0 or 1. Without loss of generality, assume that  $|d_{i,k}| = 1$  for each user  $k$  on each bandwidth  $W_i$ , and  $h_{i,b,k} = |g_{i,b,k}|^2$ . According to (3), the SINR of user  $k$  on bandwidth  $W_i$  after successful SIC is formulated as

$$\gamma_{i,k}^{\text{UNC}} = \frac{s_{i,k}}{I_{i,k}^{\text{UNC,INI}} + I_{i,k}^{\text{UNC,ICI}} + \sigma_{i,k}^2}, \quad (4)$$

where  $s_{i,k} = \sum_{b \in \mathcal{B}_i} \theta_{i,b,k} p_{i,b,k} h_{i,b,k}$  is the total received desired signal power at user  $k$  on bandwidth  $W_i$ ,  $I_{i,k}^{\text{UNC,INI}} = \sum_{\substack{k' \in \mathcal{K}, \\ \lambda_{i,k'} > \lambda_{i,k}}} \min \left\{ \sum_{b \in \mathcal{B}_i} \theta_{i,b,k} \theta_{i,b,k'}, 1 \right\} \sum_{b \in \mathcal{B}_i} \theta_{i,b,k'} p_{i,b,k'} h_{i,b,k'}$  is the received INI power at user  $k$  on bandwidth  $W_i$ , and  $I_{i,k}^{\text{UNC,ICI}} = \sum_{\substack{k' \in \mathcal{K}, \\ k' \neq k}} (1 - \min \left\{ \sum_{b \in \mathcal{B}_i} \theta_{i,b,k} \theta_{i,b,k'}, 1 \right\}) \sum_{b \in \mathcal{B}_i} \theta_{i,b,k'} p_{i,b,k'} h_{i,b,k'}$  is the received ICI power at user  $k$  on bandwidth  $W_i$ . The spectral efficiency of user  $k$  on bandwidth  $W_i$  denoted by  $r_{i,k}$  is upper-bounded by [24], [33], [36]

- 1) The Shannon's capacity for decoding the desired signal  $d_{i,k}$  after successfully decoding and canceling the signal(s) of other users in  $\Phi_{i,k}$ . Hence, we have

$$r_{i,k} \leq r_{i,k}^{\text{UNC,SE}} = \log_2 (1 + \gamma_{i,k}^{\text{UNC}}). \quad (5)$$

- 2) The Shannon's capacity for decoding and canceling the desired signal(s) of user  $k$ , i.e.,  $d_{i,k}$ , at other users with higher decoding orders within the NOMA cluster, i.e., each user  $j \in \Phi_{i,k}^{\text{INI}}$ . Hence, we have

$$\min \left\{ \sum_{b \in \mathcal{B}_i} \theta_{i,b,k} \theta_{i,b,j}, 1 \right\} r_{i,k} \leq \log_2 \left( 1 + \frac{s_{i,k,j}^{\text{VP}}}{I_{i,k,j}^{\text{UNC,VP}} + (I_{i,j}^{\text{UNC,ICI}} + \sigma_{i,j}^2)} \right), \quad \forall j \in \mathcal{K}, \lambda_{i,j} > \lambda_{i,k}, \quad (6)$$

where  $s_{i,k,j}^{\text{VP}} = \sum_{b \in \mathcal{B}_i} \theta_{i,b,k} p_{i,b,k} h_{i,b,j}$  is the decoded signal power of user  $k$  on bandwidth  $W_i$  received at user  $j$ , and  $I_{i,k,j}^{\text{UNC,VP}} = \sum_{\substack{k' \in \mathcal{K}, \\ \lambda_{i,k'} > \lambda_{i,k}}} \min \left\{ \sum_{b \in \mathcal{B}_i} \theta_{i,b,k} \theta_{i,b,k'}, 1 \right\} \sum_{b \in \mathcal{B}_i} \theta_{i,b,k'} p_{i,b,k'} h_{i,b,j}$

denotes the INI power of user  $k$  on bandwidth  $W_i$  received at user  $j$ . Note that in (6), the ICI term  $I_{i,j}^{\text{UNC,ICI}}$  is fully treated as AWGN. Hence, the term  $(I_{i,j}^{\text{UNC,ICI}} + \sigma_{i,j}^2)$  can be viewed as equivalent AWGN at user  $j$  on bandwidth  $W_i$ .

According to (5) and (6), the achievable spectral efficiency of user  $k$  on bandwidth  $W_i$  can be formulated by

$$r_{i,k} = \min \left\{ \log_2 (1 + \gamma_{i,k}^{\text{UNC}}), \min_{j \in \Phi_{i,k}^{\text{INI}}} \left\{ \log_2 \left( 1 + \frac{s_{i,k,j}^{\text{VP}}}{I_{i,k,j}^{\text{UNC,VP}} + (I_{i,j}^{\text{UNC,ICI}} + \sigma_{i,j}^2)} \right) \right\} \right\}. \quad (7)$$

In contrast to single-antenna single/multi-cell NOMA, the well-known condition  $\log_2 (1 + \gamma_{i,k}^{\text{UNC}}) \leq \min_{j \in \Phi_{i,k}^{\text{INI}}} \left\{ \log_2 \left( 1 + \frac{s_{i,k,j}^{\text{VP}}}{I_{i,k,j}^{\text{UNC,VP}} + (I_{i,j}^{\text{UNC,ICI}} + \sigma_{i,j}^2)} \right) \right\}$  does not hold at any power level. This is due to the fact that CoMP systems with arbitrary power allocation are identical to the nondegraded MISO Gaussian BCs. As a result, there is no guarantee that the rate of a user with lower decoding order for decoding its own signal be always less than the rate of decoding this signal at other users with higher decoding order. On the other hand, exploring the rate region of CoMP-NOMA needs exhaustive search which is not applicable in large-scale systems. Therefore, similar to the related works on CoMP-NOMA, we limit our study to the case that  $r_{i,k} = r_{i,k}^{\text{UNC,SE}} = \log_2 (1 + \gamma_{i,k}^{\text{UNC}})$  [2]–[4], [6], [19], [37]. According to (5)–(7), to guarantee that  $r_{i,k} = \log_2 (1 + \gamma_{i,k}^{\text{UNC}})$ ,  $\forall k \in \mathcal{K}$ ,  $i \in \mathcal{I}$ , the following SIC necessary condition should be satisfied<sup>9</sup> [38], [39]

$$\min \left\{ \sum_{b \in \mathcal{B}_i} \theta_{i,b,k} \theta_{i,b,j}, 1 \right\} r_{i,k}^{\text{UNC,SE}} \leq \log_2 \left( 1 + \frac{s_{i,k,j}^{\text{VP}}}{I_{i,k,j}^{\text{UNC,VP}} + (I_{i,j}^{\text{UNC,ICI}} + \sigma_{i,j}^2)} \right), \quad \forall i \in \mathcal{I}, \quad \forall k, j \in \mathcal{K},$$

$$\lambda_{i,j} > \lambda_{i,k}. \quad (8)$$

Fig. 3 shows an exemplary single-carrier UNC-based CoMP-NOMA system consisting of 3 BSs owned by a single InP, and 3 users with a unique decoding order  $\lambda_{1,3} > \lambda_{1,2} > \lambda_{1,1}$ . In this system, the non-CoMP-user 1 forms only one local NOMA set  $\Phi_{1,1,1}^{\text{Cell}} = \emptyset$  which is equal to its

<sup>9</sup>The main reason of imposing the SIC necessary condition on power allocation in CoMP-NOMA is to tackle the non-differentiability of (7), thus reducing the complexity of the solution algorithms which are presented in the next section.

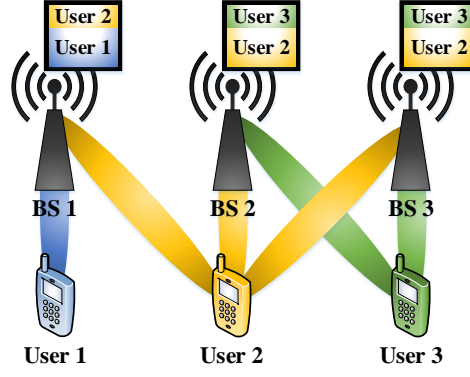


Fig. 3. A UNC-based single-carrier CoMP-NOMA system consisting of one InP including 3 BSs with 3 subscribed users. The signals with the same colour refer to the desired signals of a user.

global NOMA set  $\Phi_{1,1}$  that is empty due to the lowest decoding order. This user receives both the INI and ICI in the network. The INI power of user 1 is  $(p_{1,1,2}h_{1,1,1} + p_{1,2,2}h_{1,2,1} + p_{1,3,2}h_{1,3,1})$  since  $\theta_{1,1,1} = \theta_{1,1,2} = 1$  and  $\lambda_{1,1} < \lambda_{1,2}$ . Moreover, the ICI of user 1 is  $(p_{1,2,3}h_{1,2,1} + p_{1,3,3}h_{1,3,1})$ , because  $\sum_b \theta_{1,b,1}\theta_{1,b,3} = 0$ . Besides, CoMP-user 2 forms three local NOMA sets  $\Phi_{1,1,2}^{\text{Cell}} = \{1\}$  and  $\Phi_{1,2,2}^{\text{Cell}} = \Phi_{1,3,2}^{\text{Cell}} = \{\}$ , and subsequently a global NOMA set  $\Phi_{1,2} = \{1\}$ . Also, user 2 does not experience any ICI since  $\sum_b \theta_{1,b,2}\theta_{1,b,1}$  and  $\sum_b \theta_{1,b,2}\theta_{1,b,3}$  are nonzero. However, user 2 does experience INI power  $(p_{1,2,3}h_{1,2,2} + p_{1,3,3}h_{1,3,2})$ , due to  $\sum_b \theta_{1,b,2}\theta_{1,b,3} \geq 1$  and  $\lambda_{1,2} < \lambda_{1,3}$ . Finally, the NOMA cluster-head user 3 (with the highest decoding order) forms a global NOMA set  $\Phi_{1,3} = \{2\}$ . Since  $\lambda_{1,3} > \lambda_{1,2}$  and  $\sum_b \theta_{1,b,1}\theta_{1,b,3} = 0$ , this user does not experience any INI. However, user 3 receives ICI power  $(p_{1,1,1}h_{1,1,3})$ .

2) *Limited NOMA Clustering*: Although UNC (CoMP-NOMA protocol) provides the maximum possible interference cancellation among users, this scheme inherently increases the order of global NOMA set  $\Phi_{i,k}$  of CoMP-users, specifically when the number of CoMP-BSs increases. One disadvantage of UNC is increasing the error propagation among NOMA users. Another disadvantage is increasing the users hardware complexity, due to the larger order of NOMA



clusters. Here, we propose a LNC scheme, where for each user, the SIC is performed to the users belonging to only one of its local NOMA sets. Let  $x_{i,b,k} \in \{0, 1\}$  be the local NOMA set selection indicator, where  $x_{i,b,k} = 1$  if user  $k$  selects the local NOMA set  $\Phi_{i,b,k}^{\text{Cell}}$  on bandwidth  $W_i$ , and otherwise,  $x_{i,b,k} = 0$ . In LNC, to ensure that each user selects at most one local NOMA set on each bandwidth, the following constraint should be satisfied:

$$\sum_{b \in \mathcal{B}_i} x_{i,b,k} \leq 1, \forall i \in \mathcal{I}, k \in \mathcal{K}. \quad (9)$$

According to the NOMA protocol, user  $k$  can select the local NOMA set of BS  $b \in \mathcal{B}_i$  on bandwidth  $W_i$  if it is associated with that BS. Therefore, we have

$$x_{i,b,k} \leq \theta_{i,b,k}, \forall i \in \mathcal{I}, b \in \mathcal{B}_i, k \in \mathcal{K}. \quad (10)$$

Let  $x_{i,b,k} = \theta_{i,b,k} = 1$ . According to the LNC protocol, user  $k$  decodes and cancels the signal(s) of user  $k'$  if  $k' \in \Phi_{i,b,k}^{\text{Cell}}$ , or equivalently,  $\theta_{i,b,k'} = 1$  and  $\lambda_{i,k} > \lambda_{i,k'}$ . The signal(s) of user  $k'$  is treated as INI at user  $k$  if  $\theta_{i,b,k'} = 1$  and  $\lambda_{i,k'} > \lambda_{i,k}$ . Moreover, the signal(s) of user  $k'$  is treated as ICI at user  $k$  if  $\theta_{i,b,k'} = 0$ . As a result, the signal(s) of users who are not associated to the selected cell are fully treated as noise (called ICI). Actually, LNC can be viewed as CoMP-NOMA with partial SIC in which the interference cancellation of NOMA is considered to a subset of potential users (with lower decoding order) within the NOMA cluster. Obviously, since each non-CoMP-user is associated to only one BS, i.e.,  $|\mathcal{C}_{i,k}| = 1$ , it has only one local NOMA set. As a result, the non-CoMP-user can only select the local NOMA set of its associated cell, due to the multi-cell NOMA protocol. Therefore, the SINR expression of users in traditional multi-cell NOMA systems (without CoMP) in LNC and UNC is the same. On the other hand, each CoMP-user has multiple local NOMA clusters. According to the LNC protocol, the local NOMA set selection is challenging for only the CoMP-users. Among these users, the local NOMA set selection is more challenging for the CoMP-users with higher decoding order. For instance, in Fig. 3, with another predefined SIC ordering  $\lambda_{1,2} > \lambda_{1,3} > \lambda_{1,1}$  for LNC, if user 2 selects  $\Phi_{1,2,2}^{\text{Cell}} = \{3\}$ , it decodes and cancels the signals of user 3 (because  $\theta_{1,2,2}\theta_{1,2,3} = 1$ ).

However, user 2 receives ICI power  $(p_{1,1,1}h_{1,1,2})$  since  $\theta_{1,2,2}\theta_{1,2,1} = 0$ . Besides, if user 2 selects  $\Phi_{1,1,2}^{\text{Cell}} = \{1\}$ , it receives ICI power  $(p_{1,2,3}h_{1,2,2} + p_{1,3,3}h_{1,3,2})$  since  $\theta_{1,1,2}\theta_{1,1,3} = 0$ .

The INI and ICI at users are highly affected by the local NOMA set selection of CoMP-users. Accordingly,  $x_{i,b,k}$  needs to be determined jointly with power allocation and user association. After successful SIC, the received signal of user  $k$  on bandwidth  $W_i$  in LNC is given by

$$y_{i,k} = \underbrace{\sum_{b \in \mathcal{B}_i} \theta_{i,b,k} \sqrt{p_{i,b,k}} g_{i,b,k} d_{i,k}}_{\text{desired signal}} + \underbrace{\sum_{\substack{k' \in \mathcal{K}, \\ \lambda_{i,k'} > \lambda_{i,k}}} \sum_{b \in \mathcal{B}_i} x_{i,b,k} \theta_{i,b,k'} \sum_{b' \in \mathcal{B}_i} \theta_{i,b',k'} \sqrt{p_{i,b',k'}} g_{i,b',k} d_{i,k'}}_{\text{INI}} + \underbrace{\sum_{\substack{k' \in \mathcal{K}, \\ k' \neq k}} \sum_{b \in \mathcal{B}_i} x_{i,b,k} (1 - \theta_{i,b,k'}) \sum_{b' \in \mathcal{B}_i} \theta_{i,b',k'} \sqrt{p_{i,b',k'}} g_{i,b',k} d_{i,k'}}_{\text{ICI}} + N_{i,k}, \quad (11)$$

where the first term is the received desired signal at user  $k$ , and the second and third terms are the INI and ICI at user  $k$ , respectively. After successful SIC at users, the SINR of user  $k$  on bandwidth  $W_i$  is given by

$$\gamma_{i,k}^{\text{LNC}} = \frac{S_{i,k}}{I_{i,k}^{\text{LNC,INI}} + I_{i,k}^{\text{LNC,ICI}} + \sigma_{i,k}^2}, \quad (12)$$

where  $I_{i,k}^{\text{LNC,INI}} = \sum_{\substack{k' \in \mathcal{K}, \\ \lambda_{i,k'} > \lambda_{i,k}}} \sum_{b \in \mathcal{B}_i} x_{i,b,k} \theta_{i,b,k'} \sum_{b' \in \mathcal{B}_i} \theta_{i,b',k'} p_{i,b',k'} h_{i,b',k}$  is the INI at user  $k$  on bandwidth  $W_i$ , and  $I_{i,k}^{\text{LNC,ICI}} = \sum_{\substack{k' \in \mathcal{K}, \\ k' \neq k}} \sum_{b \in \mathcal{B}_i} x_{i,b,k} (1 - \theta_{i,b,k'}) \sum_{b' \in \mathcal{B}_i} \theta_{i,b',k'} p_{i,b',k'} h_{i,b',k}$  is the ICI at user  $k$  on bandwidth  $W_i$ . According to (9)-(12), the spectral efficiency of user  $k$  on bandwidth  $W_i$  after successful SIC is given by  $r_{i,k}^{\text{LNC,SE}} = \log_2 (1 + \gamma_{i,k}^{\text{LNC}})$ . Similar to UNC, we assume that the spectral efficiency of each user is obtained by  $r_{i,k}^{\text{LNC,SE}}$ . Similar to (8), the following SIC necessary constraint should be satisfied:

$$x_{i,b,k} \theta_{i,b,j} r_{i,k}^{\text{LNC,SE}} \leq \log_2 \left( 1 + \frac{S_{i,k,j}^{\text{VP}}}{I_{i,k,j}^{\text{LNC,VP}} + (I_{i,j}^{\text{LNC,ICI}} + \sigma_{i,j}^2)} \right), \quad \forall i \in \mathcal{I}, b \in \mathcal{B}_i, k, j \in \mathcal{K}, \lambda_{i,j} > \lambda_{i,k}, \quad (13)$$

where  $I_{i,k,j}^{\text{LNC,VP}} = \sum_{\substack{k' \in \mathcal{K}, \\ \lambda_{i,k'} > \lambda_{i,k}}} \sum_{b \in \mathcal{B}_i} x_{i,b,k} \theta_{i,b,k'} \sum_{b' \in \mathcal{B}_i} \theta_{i,b',k'} p_{i,b',k'} h_{i,b',j}$  denotes the INI power of user  $k$

on bandwidth  $W_i$  received at user  $j$ . The term  $s_{i,k,j}^{\text{VP}} = \sum_{b \in \mathcal{B}_i} \theta_{i,b,k} p_{i,b,k} h_{i,b,j}$  is the signal power of user  $k$  received at user  $j$  (which is the same as  $s_{i,k,j}^{\text{VP}}$  in (8)).

### C. SIC Ordering in SV-CoMP-NOMA

According to the rate region of users in CoMP-NOMA (see (7)), the optimal SIC ordering depends on both the ICI and received signal strength at users. For the case that  $r_{i,k} = r_{i,k}^{\text{UNC,SE}} = \log_2(1 + \gamma_{i,k}^{\text{UNC}})$ , the optimal decoding order for maximizing total spectral efficiency of users can be obtained by (8). However, the optimal decoding order is still challenging, due to the existing ICI (which is treated as AWGN) [33], [34], [36] and signal strength at users (due to the nondegradation of CoMP with arbitrary power allocation which is identical to the MISO Gaussian BCs with PAPC) [2], [3], [18], [19]. One solution is to examine all the possible decoding orders among users [3]. However, the complexity of this algorithm will be exponential in the number of users when the user association is not predefined in the SIC decoding order. In the following, we find a suboptimal decoding order based on only the channel gains of users.

Assume that each user is connected to all the BSs over each bandwidth  $W_i$ , i.e.,  $\theta_{i,b,k} = 1$ ,  $\forall k \in \mathcal{K}$ ,  $b \in \mathcal{B}_i$ . Then, we have  $\mathcal{C}_{i,k} = \mathcal{B}_i$  for each user  $k$ , and subsequently,  $\mathcal{C}_{i,k} \cap \mathcal{C}_{i,k'} \neq \emptyset$  or equivalently  $\sum_{b \in \mathcal{B}_i} \theta_{i,b,k} \theta_{i,b,k'} \geq 1$  for each user pair  $(k, k')$ . In this case, we have a single  $K$ -order NOMA cluster with  $B_i = |\mathcal{B}_i|$  CoMP-BSs transmitting signals to each user over each bandwidth  $W_i$ . Each user is thus a CoMP-user. Assume that the decoding order  $j > k$ ,  $\lambda_{i,j} > \lambda_{i,k}$  is applied. According to (4), the SINR of user  $k$  can be obtained by

$$\gamma_{i,k} = \frac{\sum_{b \in \mathcal{B}_i} p_{i,b,k} h_{i,b,k}}{\sum_{k'=k+1} \sum_{b \in \mathcal{B}_i} p_{i,b,k'} h_{i,b,k} + \sigma_{i,k}^2}. \quad (14)$$

This system can be viewed as a distributed antenna system including a single super-BS transmitting signals to  $K$  users. In this system, the ICI is zero while each user may experience INI depending on the decoding order. According to (8), the decoding order  $j > k \Rightarrow \lambda_{i,j} > \lambda_{i,k}$  is

optimal independent from power allocation if and only if for the user pair  $(k, j)$ , the condition

$$\frac{\sum_{b \in \mathcal{B}_i} p_{i,b,k} h_{i,b,k}}{\sum_{k'=k+1} \sum_{b \in \mathcal{B}_i} p_{i,b,k'} h_{i,b,k} + \sigma_{i,k}^2} \leq \frac{\sum_{b \in \mathcal{B}_i} p_{i,b,k} h_{i,b,j}}{\sum_{k'=k+1} \sum_{b \in \mathcal{B}_i} p_{i,b,k'} h_{i,b,j} + \sigma_{i,j}^2}, \quad (15)$$

holds independent from power allocation. As is mentioned, the condition in (15) depends on power allocation in general, thus the optimality of the latter decoding order cannot be guaranteed before power allocation. For the case that BSs allocate the same power level to each user [6], i.e., for each user  $k$  over each bandwidth  $W_i$ ,  $p_{i,b,k} = p_{i,b',k}$ ,  $\forall b, b' \in \mathcal{B}_i$ , the received signal power at user  $k$  can be obtained by  $\sum_{b \in \mathcal{B}_i} p_{i,b,k} h_{i,b,k} = p_{i,b,k} \left( \sum_{b \in \mathcal{B}_i} h_{i,b,k} \right) = q_{i,k} \hat{h}_{i,k}$ , where  $\hat{h}_{i,k} = \sum_{b \in \mathcal{B}_i} h_{i,b,k}$  is the equivalent channel gain from the super-BS to user  $k$  on bandwidth  $W_i$ , and  $q_{i,k} = p_{i,b,k}$  is the allocated power to user  $k$  at each BS  $b \in \mathcal{B}_i$ . According to the above, the general CoMP-NOMA model is simplified to  $I$  single-antenna single-cell NOMA systems each having a single super-BS operating in an isolated bandwidth. The SINR of user  $k$  on bandwidth  $W_i$  can be formulated by

$$\gamma_{i,k} = \frac{\sum_{b \in \mathcal{B}_i} q_{i,k} \hat{h}_{i,k}}{\sum_{k'=k+1} \sum_{b \in \mathcal{B}_i} q_{i,k'} \hat{h}_{i,k} + \sigma_{i,k}^2}. \quad (16)$$

The rest of the analysis for each super-BS is the same as single-cell NOMA. The decoding order  $\lambda_{i,j} > \lambda_{i,k}$  results in maximum total spectral efficiency, so is optimal, if and only if

$$\frac{\sum_{b \in \mathcal{B}_i} q_{i,k} \hat{h}_{i,k}}{\sum_{k'=k+1} \sum_{b \in \mathcal{B}_i} q_{i,k'} \hat{h}_{i,k} + \sigma_{i,k}^2} \leq \frac{\sum_{b \in \mathcal{B}_i} q_{i,k} \hat{h}_{i,j}}{\sum_{k'=k+1} \sum_{b \in \mathcal{B}_i} q_{i,k'} \hat{h}_{i,j} + \sigma_{i,j}^2}, \quad (17)$$

for any  $\mathbf{q} = [q_{i,k}]$ . The inequality in (17) can be rewritten as  $\frac{\hat{h}_{i,k}}{\sigma_{i,k}} \leq \frac{\hat{h}_{i,j}}{\sigma_{i,j}}$ . Therefore, the decoding order  $\lambda_{i,j} > \lambda_{i,k}$  is optimal if and only if  $\frac{\hat{h}_{i,k}}{\sigma_{i,k}} \leq \frac{\hat{h}_{i,j}}{\sigma_{i,j}}$ . Our suboptimal decoding order follows the ascending order of users equivalent channel gain  $(\hat{h}_{i,k})$  normalized by noise. The equivalent channel gain of each user is the positive summation of all the channel gains from BSs to the user. The performance of this decoding order is evaluated in Subsection IV-A.

#### D. Problem Formulations

In this network, the amount of bandwidth  $W_i$  may be different for each InP. In this way, the overall spectral efficiency of a user connected to different InPs would not correspond to its overall data rate. Here, we assume that the revenue of each MVNO comes from providing data rates for its subscribed users [9], [40] such that  $\omega_v$  units/bps denotes the unit price of revenue of MVNO  $v$  due to providing data rates for users in  $\mathcal{K}_v$ . In the following, we formulate the problem of maximizing total revenue of MVNOs corresponding to the weighted sum-rate of users. The data rate of user  $k$  in the UNC and LNC schemes can be obtained by  $r_k^{\text{UNC}} = \sum_{i \in \mathcal{I}} W_i r_{i,k}^{\text{UNC,SE}}$  and  $r_k^{\text{LNC}} = \sum_{i \in \mathcal{I}} W_i r_{i,k}^{\text{LNC,SE}}$ , respectively. The UNC problem is formulated as follows:

$$\text{UNC: } \max_{\mathbf{p}, \boldsymbol{\theta}} \sum_{v \in \mathcal{V}} \sum_{k \in \mathcal{K}_v} \omega_v r_k^{\text{UNC}} \quad (18a)$$

$$\text{s.t. (8),}$$

$$r_k^{\text{UNC}} \geq R_v^{\text{rsv}}, \forall v \in \mathcal{V}, k \in \mathcal{K}_v, \quad (18b)$$

$$\sum_{k \in \mathcal{K}} p_{i,b,k} \leq P_{i,b}^{\text{max}}, \forall i \in \mathcal{I}, b \in \mathcal{B}_i, \quad (18c)$$

$$\sum_{b \in \mathcal{B}_i} \theta_{i,b,k} \leq \Psi_i^{\text{max}}, \forall i \in \mathcal{I}, k \in \mathcal{K}, \quad (18d)$$

$$\theta_{i,b,k} \in \{0, 1\}, \forall i \in \mathcal{I}, b \in \mathcal{B}_i, k \in \mathcal{K}, \quad (18e)$$

$$p_{i,b,k} \geq 0, \forall i \in \mathcal{I}, b \in \mathcal{B}_i, k \in \mathcal{K}, \quad (18f)$$

where  $\mathbf{p} = [p_{i,b,k}]$  and  $\boldsymbol{\theta} = [\theta_{i,b,k}]$ . Constraint (8) is the SIC necessary condition for successful SIC at users in the UNC model. Furthermore, (18b) is the minimum required data rate constraint of user  $k \in \mathcal{K}_v$ , and (18c) is the maximum available power constraint of each BS. Moreover, (18d) indicates that each user  $k \in \mathcal{K}$  can be associated to at most  $\Psi_i^{\text{max}}$  BSs in InP  $i$  [3]. The main advantages of restricting the order of CoMP-BSs for each CoMP-user are listed as follows: 1) alleviating the backhaul traffic, due to the joint transmission of CoMP [41]; 2)

reducing the complexity of synchronization at CoMP-BSs; 3) decreasing the order of NOMA clusters which reduces: 1. error propagation in CoMP-NOMA; 2. SIC complexity at CoMP-users; 3. superposition coding at CoMP-BSs; 4. the negative side effect of SIC on users spectral efficiency [3], [19]. The LNC problem is formulated as

$$\text{LNC: } \max_{\mathbf{p}, \boldsymbol{\theta}, \mathbf{x}} \sum_{v \in \mathcal{V}} \sum_{k \in \mathcal{K}_v} \omega_v r_k^{\text{LNC}} \quad (19a)$$

$$\text{s.t. (9), (10), (13), (18c)-(18f),}$$

$$r_k^{\text{LNC}} \geq R_v^{\text{rsv}}, \forall v \in \mathcal{V}, k \in \mathcal{K}_v, \quad (19b)$$

$$x_{i,b,k} \in \{0, 1\}, \forall i \in \mathcal{I}, b \in \mathcal{B}_i, k \in \mathcal{K}, \quad (19c)$$

where  $\mathbf{x} = [x_{i,b,k}]$ ,  $\forall i \in \mathcal{I}, b \in \mathcal{B}_i, k \in \mathcal{K}$ . Compared to the UNC problem, LNC adds a new binary optimization variable  $\mathbf{x}$  with two integer linear inequality constraints (9) and (10).

### III. JOINT POWER ALLOCATION AND USER ASSIGNMENT ALGORITHMS

The problems (18) and (19) are classified as MINLP which are intractable and NP-hard [3], [35], [37]. Additionally, the existing optimal solutions for single-cell or multi-cell NOMA systems cannot be directly applied to the CoMP-NOMA systems [3].

#### A. Solution Algorithms for the UNC Problem

1) *Global Optimality: Mixed-Integer Monotonic Optimization:* Here, we find a globally optimal solution for the problem (18) by proposing a mixed-integer monotonic program. The basic idea of the monotonic optimization is reducing the exploration area for finding the globally optimal solution of a monotonic problem to its outer boundary which reduces the computational complexity, and provides a guaranteed convergence. The monotonic optimization can solve problems, where the objective function is monotone and constraints are the intersection of normal and co-normal sets [38], [42]. A monotonic optimization problem in canonical form

can be formulated by

$$\max_{\mathbf{x} \in \mathbb{R}^N} f(\mathbf{x}) \quad \text{s.t. } \mathbf{x} \in \mathcal{S} \cap \mathcal{S}_c, \quad (20)$$

where the objective function  $f(\mathbf{x}) : \mathbb{R}^N \rightarrow \mathbb{R}$  is increasing in  $\mathbf{x}$ . The set  $\mathcal{S} = \{\mathbf{x} \in \mathbb{R}^N : g(\mathbf{x}) \leq 0\}$  is a compact, normal set with nonempty interior, and the set  $\mathcal{S}_c = \{\mathbf{x} \in \mathbb{R}^N : h(\mathbf{x}) \geq 0\}$  is a closed co-normal set. For more details, please see Subsection III-B in [42]. In Proposition 7 in [43], it is proved that the solution of (20) lies on the upper boundary of  $\mathcal{S} \cap \mathcal{S}_c$ . In this regard, the methods like the poly block [43] and branch-reduce-and-bound [44] algorithms can be utilized to find the globally optimal solution. Thus, the only challenge is how to transform the main problem to a monotonic optimization problem in canonical form [42]. Problem (18) is not a monotonic problem in canonical form because of the following issues: 1) The user association variable  $\theta$  in (18e) results in a non-continuous domain in (18); 2) The rate function in (18a) and (18b) cannot be directly transformed to the difference of two increasing functions, because of the non-increasing term  $(1 - \min \{ \sum_{b \in \mathcal{B}_i} \theta_{i,b,k} \theta_{i,b,k'}, 1 \})$  in  $I_{i,k}^{\text{UNC,ICI}}$  in (4) with respect to  $\theta$ ; 3) The objective function (18a) is not monotonic, since the SINR fraction in (4) is increasing neither in  $\mathbf{p}$  nor in  $\theta$ ; 4) The constraint sets in (8) and (18b) are not guaranteed to be the intersection of normal and co-normal sets, since the difference of two increasing functions is in general nonincreasing. However, (18) shows a hidden monotonicity structure after issues 1 and 2 are solved. In Appendix A, we transform (18) to a monotonic program in canonical form. The transformed problem can be easily solved by using the poly block or branch-reduce-and-bound algorithms.

2) *First-Order Optimality: Sequential Programming:* Despite the global optimality of the proposed mixed-integer monotonic program, the complexity of this method is still exponential in the number of optimization variables. Indeed, this algorithm can be considered as a benchmark for any low-complexity yet suboptimal method. Here, we apply the SCA algorithm which is a locally optimal solution with a polynomial time complexity [22], [35], [40], [45], [46]. Note

---

**Algorithm 1** SCA with DC programming.

---

1: Initialize  $\boldsymbol{\vartheta}^{(0)}$ , and penalty factor  $\eta \gg 1$ .

**repeat**

2: Find  $\boldsymbol{\vartheta}^{(l)}$  by solving the convex approximated form of (49) for a given  $\boldsymbol{\vartheta}^{\text{old}}$ .

3: Set  $\boldsymbol{\vartheta}^{\text{old}} = \boldsymbol{\vartheta}^{(l)}$ , and store it.

4: Set  $l = l + 1$

**Until** Convergence of (49a).

5:  $\boldsymbol{\vartheta}^* = \boldsymbol{\vartheta}^{(l)}$  is the output of the algorithm.

6:  $\boldsymbol{\theta}^*$  and  $\boldsymbol{p}^*$  are adopted for the network.

---

that the SCA algorithm cannot be directly applied to (18), because of: 1) Combinatorial nature of (18), due to binary variable  $\boldsymbol{\theta}$ ; 2) Multiplication of  $\boldsymbol{\theta}$  and  $\boldsymbol{p}$  in the objective function (18a), and constraints (8) and (18b) (please see (4)); 3) The term  $(1 - \min\{.\})$  in (4) with respect to  $\boldsymbol{\theta}$ ; 4) The term  $\theta_{i,b,k}\theta_{i,b,k'}$  in  $\min\{\sum_{b \in \mathcal{B}_i} \theta_{i,b,k}\theta_{i,b,k'}, 1\}$  and  $(1 - \min\{\sum_{b \in \mathcal{B}_i} \theta_{i,b,k}\theta_{i,b,k'}, 1\})$  (please see (4)); 5) Multiplications of  $\min\{\sum_{b \in \mathcal{B}_i} \theta_{i,b,k}\theta_{i,b,k'}, 1\}$  and  $(1 - \min\{\sum_{b \in \mathcal{B}_i} \theta_{i,b,k}\theta_{i,b,k'}, 1\})$  with  $\theta_{i,b,k'}p_{i,b,k'}$  in (4). However, (18) can be transformed into an equivalent form which can be solved by directly applying the SCA algorithm. The series of equivalent transformations of this MINLP problem is presented in Appendix B. After these transformations, we apply the SCA algorithm with the difference of convex (DC) approximation method to the transformed nonconvex problem as follows: We first initialize the approximation parameters. After that, the convex approximated problem is solved. These iterations are repeated until the convergence is achieved. The pseudo code of the SCA algorithm is presented in Alg. 1. The derivations of SCA for solving the transformed problem (49) is presented in Appendix C. Moreover, we analytically show that the proposed SCA algorithm generates a sequence of improved solutions in Appendix D. Hence, we prove that SCA converges to a stationary point which is a local maximum of (18).



### B. Solution Algorithms for the LNC Problem

1) *Global Optimality: Mixed-Integer Monotonic Optimization:* The problems (18) and (19) have similar structure and nonconvexity challenges. Hence, to find a globally optimal solution for (19), we modify our proposed mixed-integer monotonic optimization for solving (18) to be applied to (19). In this line, we show how (19) can be equivalently transformed into a monotonic optimization problem in canonical form in Appendix E.

2) *First-Order Optimality: Sequential Programming:* Since (18) and (19) have the same structure, the proposed SCA algorithm for solving (19) is similar to that of proposed for solving (18). Due to the space limitation, the presentation of the proposed SCA algorithm with DC programming for solving (19) is not included here. It can be easily proved that this algorithm also converges to a locally optimal solution.

## IV. SIMULATION RESULTS

In this section, we first compare the performance of suboptimal and optimal decoding orders in two small-scale networks. Then, we investigate the performance of our proposed UNC and LNC schemes in the SV-CoMP-NOMA system with different resource allocation strategies.

### A. Performance of Suboptimal Decoding Order

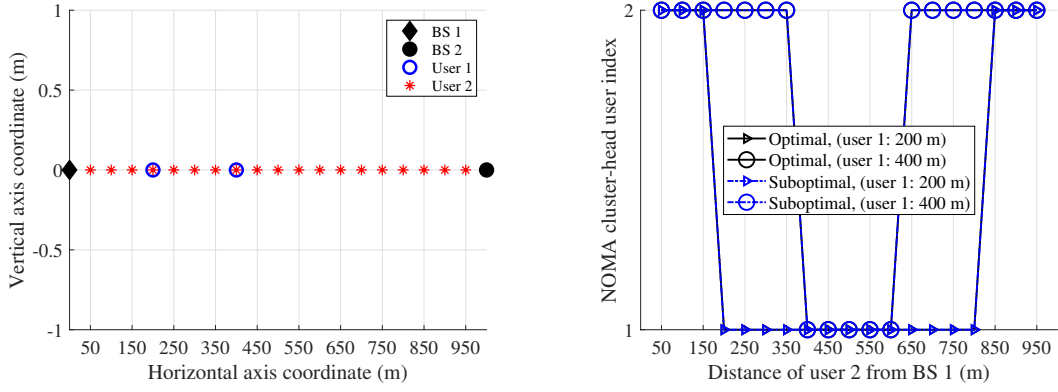
Here, we compare the performance (in terms of total spectral efficiency) of our suboptimal decoding order (discussed in Subsection II-C) with the optimal decoding order. The optimal decoding order is achieved by exploring all the possible decoding orders among users. To have a fair comparison, we adopt optimal power allocation among users based on the exhaustive search method. We also explore the rate region of CoMP-NOMA such that the spectral efficiency of each user is obtained by (7). Here, we consider a simple 2-BS scenario with 2 users. The optimal user association is determined through power allocation optimization. We assume that both the users are potential CoMP-users. The performance gap between these two decoding orders is

highly affected by the channel gain differences among users. Similar to single-cell NOMA, the large-scale fading acts as an important role on this performance gap [24]. Therefore, we evaluate this performance gap in different positions of users in the direct line between two BSs. In the following, we compared the performance of optimal and suboptimal decoding orders for two environments: 1) A homogeneous network including 2 macro BSs (MBSs) (Fig. 4); 2) A HetNet including one MBS and one femto BS (FBS) (Fig. 5).

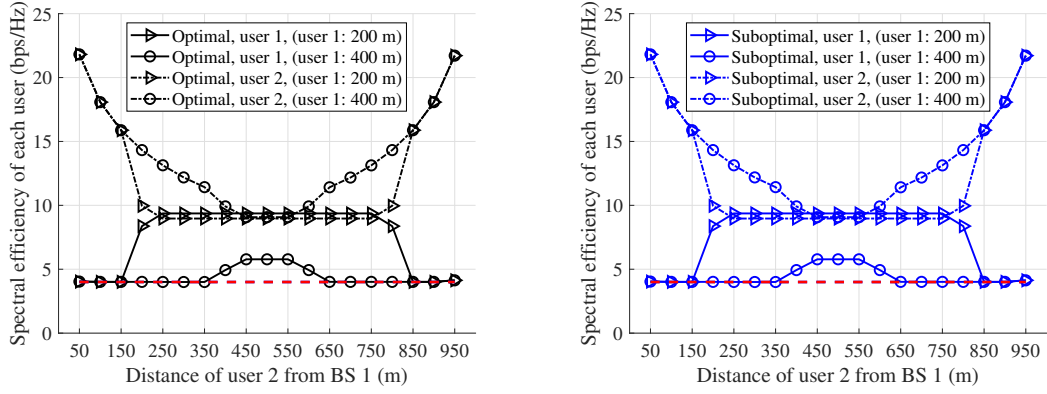
In the homogeneous network (Fig. 4), we assume that there are two MBSs with a distance 1000 m. The distances of users 1 and 2 to BS 1 are  $\{200, 400\}$  m, and  $\{50, 100, 150, 200, \dots, 950\}$  m, respectively. The network topology and different positions of each user are shown in Fig. 4(a). The channel gain includes path loss modeled as  $128.1 + 37.6 \log_{10}(d_{i,j})$  dB, where  $d_{i,j}$  is the distance between BS  $i$  and user  $j$  in km. The AWGN power is  $-114$  dBm. The MBS maximum power is  $P_b^{\max} = 46$  dBm. The minimum rate of each user is set to 4 bps/Hz. The step-size of exhaustive search is  $P_b^{\max}/10^3$  Watts. Fig. 4(b) shows which user is the NOMA cluster-head user. The NOMA cluster-head user (with higher decoding order) is the user which cancels the signal(s) of other user. Figs. 4(c) and 4(d) show the spectral efficiency of each user in optimal and suboptimal decoding orders, respectively. Finally, Fig. 4(e) shows the total spectral efficiency for the optimal and suboptimal decoding orders. As can be seen in Fig. 4(b), the NOMA cluster-head user is the same in optimal and suboptimal decoding orders at every users position. This is because, the channel gain differences among users play an important role in optimal decoding orders. As a result, the rate region of users in optimal and suboptimal decoding orders is the same (see Figs. 4(c) and 4(d)) resulting in the same total spectral efficiency performance.

In the HetNet (Fig. 5), we assume that users are distributed in the coverage area of FBS with radii of<sup>10</sup> 100 m. The distance between MBS and FBS is 200 m. The distances of users 1 and

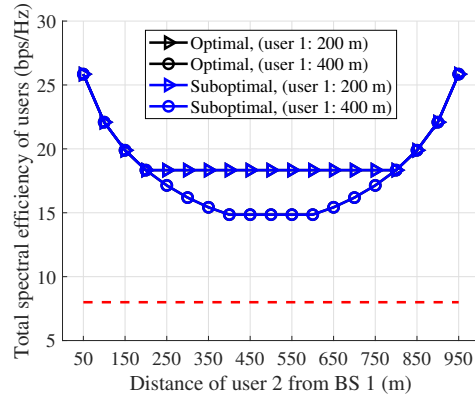
<sup>10</sup>Here, we considered a larger coverage area for FBS to have a comprehensive observation on the impact of users positions on the performance gap between optimal and suboptimal decoding orders.



(a) The network topology and different positions of users. (b) NOMA cluster-head user index in optimal and suboptimal decoding orders.



(c) Achievable spectral efficiency of each user for the optimal decoding order. (d) Achievable spectral efficiency of each user for the suboptimal decoding order.

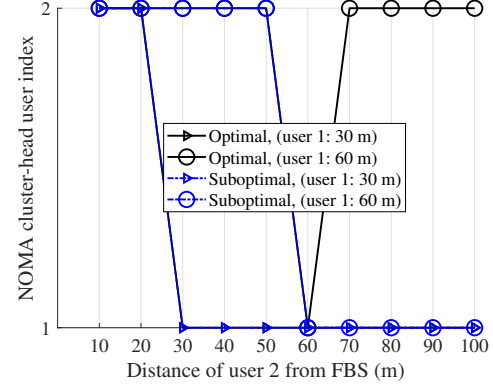
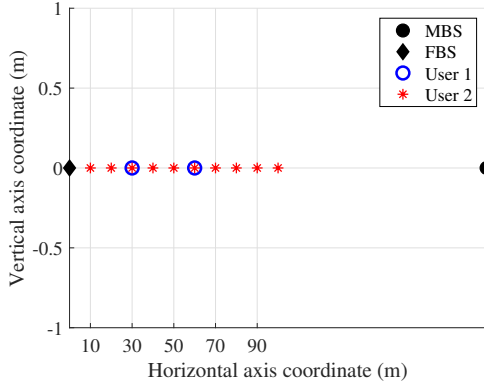


(e) Total spectral efficiency of users for the optimal and suboptimal decoding orders.

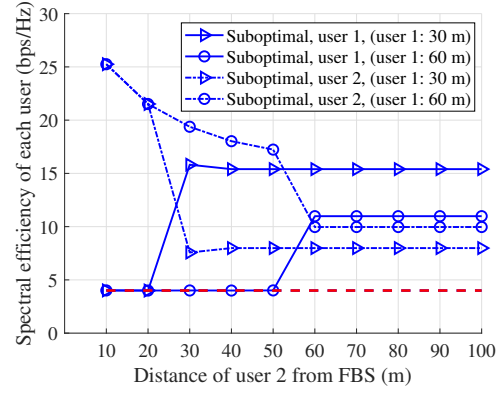
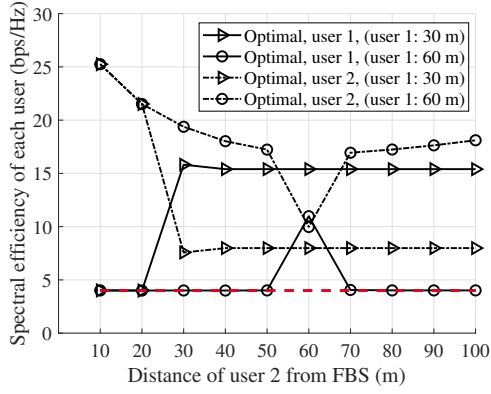
Fig. 4. Homogeneous Network: Spectral efficiency of users vs. distance of user 2 from BS 1 for different distances of user 1 to BS 1

2 to FBS are  $\{30, 60\}$  m, and  $\{10, 20, 30, \dots, 100\}$  m, respectively. The network topology and different positions of each user are shown in Fig. 5(a). The rest of the simulation settings is the same as the settings in Fig. 4. The FBS power is 30 dBm. The description of sub-figures in Fig. 5 is the same as Fig. 4. In contrast to the homogeneous network, in Fig. 5(b), we observe that when user 1 has larger distance to FBS (e.g., 60 m to FBS) and user 2 is more closer to MBS than user 1 (e.g., user 2 is more than 70 m to FBS or equivalently less than 130 m to MBS), the decoding order between optimal and suboptimal methods is different. This difference results in lower total spectral efficiency of suboptimal decoding order shown in Fig. 5(e). For the case that users 1 and 2 have 60 and 100 meters distance to the FBS, respectively, the optimal and suboptimal decoding orders have the largest performance gap nearly 5%. Although we cannot guarantee the optimality of the decoding order based on the equivalent channel gains  $\hat{h}_k = \sum_{b=1}^2 h_{b,k}$  normalized by noise, the results show that the suboptimal decoding order with negligible complexity has a near-to-optimal performance, so is a good and reasonable solution. The low performance gap between suboptimal and optimal decoding orders is due to the following reasons:

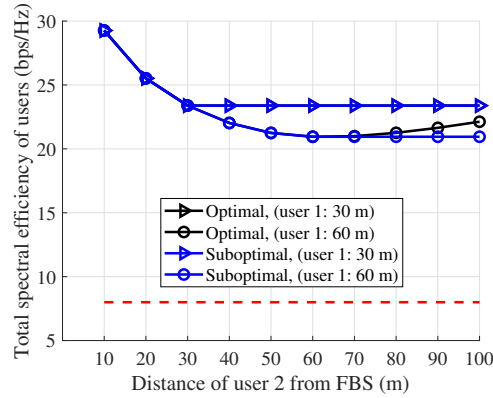
- 1) For the cell-center user  $k$ , one channel gain among  $\{h_{1,k}, \dots, h_{B,k}\}$  is dominant in  $\hat{h}_k$  compared to the other channel gains. Due to the large-scale fading, for the cell-center user which is near to BS 1, we have  $h_{1,k} \gg h_{2,k}$ . Hence,  $\hat{h}_k = \sum_{b=1}^2 h_{b,k} \cong h_{1,k}$ . As a result, the user association does not have significant impact on the equivalent channel gains of users.
- 2) The cell-center user receives stronger power than the cell-edge users. The best channel gain of the cell-center user is on the order of  $10^{-6} \sim 10^{-8}$  while the cell-edge user suffers from poor channel conditions which are on the order of  $10^{-10} \sim 10^{-13}$ . As a result, the cell-edge user still receives weaker signal power compared to the cell-center users, even for the case that the cell-edge user is a CoMP-user and the cell-center user is a non-CoMP-user [3]. Therefore, regardless of the joint transmission of CoMP, the cell-center user usually has a higher decoding order than each cell-edge user. Following Reason 1,



(a) The network topology and different positions of users. (b) NOMA cluster-head user index in optimal and suboptimal decoding orders.



(c) Achievable spectral efficiency of each user for the optimal decoding order. (d) Achievable spectral efficiency of each user for the suboptimal decoding order.



(e) Total spectral efficiency of users for the optimal and suboptimal decoding orders.

Fig. 5. Heterogeneous Network: Spectral efficiency of users vs. distance of user 2 from FBS for different distances of user 1

the decoding order between cell-center and cell-edge users (with significant channel gain differences) is approximately the same in the suboptimal and optimal decoding orders.

- 3) The optimal decoding order is challenging when the channel gain differences is quite low. This case corresponds to the optimal decoding order among two nearby cell-edge users. In this case, the user association and power allocation (and subsequently signal strength) may affect the decoding order of these nearby users with poor channel conditions. And, the suboptimal and optimal decoding orders may not be the same. Based on the rate region of users in CoMP-NOMA (see (7)), the lower channel gain differences in a user pair results in lower performance gap (total spectral efficiency gap) between different decoding orders. For the case that the channel gain differences tends to zero, the performance gap tends to zero. In this situation, different decoding orders results in the same total spectral efficiency. As a result, the optimal decoding order among cell-edge users with low channel gain differences is more challenging but not necessary.

### *B. Simulation Settings*

Here, we consider 2 InPs each having one MBS and 4 FBSs. We assume that the BSs of different InPs are co-located. Actually, we have a virtual MBS (VMBS) and 4 virtual FBSs (VFBSs). The VMBS is positioned at the center of a circular area, and VFBSs are positioned in coordinates (femto-cells)  $300\angle 0^\circ$ ,  $300\angle 22.5^\circ$ ,  $300\angle 67.5^\circ$ , and  $300\angle 90^\circ$  [45]. Assume that 6 users are uniformly (and independently) distributed in the area of each femto-cell with radii of 80 m [6]. Fig. 6 shows the network topology with an exemplary user placement.

Following the Third Generation Partnership Project (3GPP) Long Term Evolution-Advanced (LTE-A), the orthogonal wireless bandwidth of each InP is set to  $W_i = 20$  MHz with a carrier frequency of 2 GHz [8]. The wireless fading channels include both the large-scale and small-scale fading. The large-scale fading is modeled as  $128.1 + 37.6 \log_{10} d_{i,b,k}$  in dB, where  $d_{i,b,k}$  is the distance from BS  $b \in \mathcal{B}_i$  to user  $k$  in km [3]. The small-scale fading is modeled as

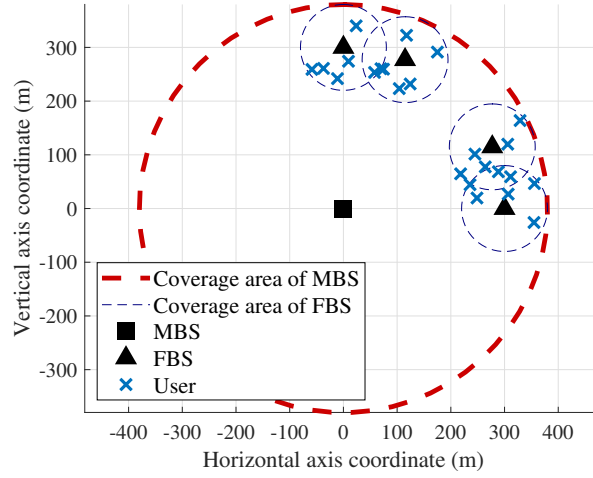


Fig. 6. Network topology and exemplary user placement in the numerical results.

independent and identically distributed (i.i.d.) Rayleigh fading with zero mean and variance one. The power spectral density (PSD) of AWGN is -174 dBm/Hz [22]. The transmit power of each MBS and each FBS are set to 46 dBm and 30 dBm, respectively [3]. Without loss of generality, we assume that the minimum required data rate of users is 8 Mbps<sup>11</sup>. Then, we set  $\omega_v = 1$  unit/bps for each  $v \in \mathcal{V}$ .

In the following, we investigate the performance of our proposed UNC and LNC schemes in different NOMA systems equipped with/without WNV and CoMP. To this end, we investigate the performance gains of WNV and CoMP by comparing our proposed SV-CoMP-NOMA system with the following systems:

- **Non-Virtualized CoMP (NoWNV-CoMP):** In this system, each user can be associated to only one InP, due to the isolation among InPs (see Subsection II-A). Therefore, constraint (1) is added to the resource allocation problems.

<sup>11</sup>In our system, WNV breaks the isolation between InPs. Therefore, the number of MVNOs does not impact on the system performance when all the users have the same SLAs and rewards.

- Virtualized Non-CoMP (WNV-NoCoMP): In this system, each user can be associated to only one BS at each InP. Hence, the joint transmission of CoMP is eliminated. However, each user could benefit from the multi-connectivity opportunity. In this way, the following constraint should be satisfied:  $\sum_{b \in \mathcal{B}_i} \theta_{i,b,k} \leq 1, \forall i \in \mathcal{I}, k \in \mathcal{K}$ .
- Non-Virtualized Non-CoMP (NoWNV-NoCoMP): In this system, each user can be associated to only one BS through the network. Hence, the following constraint should be satisfied:

$$\sum_{i \in \mathcal{I}} \sum_{b \in \mathcal{B}_i} \theta_{i,b,k} \leq 1, \forall k \in \mathcal{K}.$$

To investigate the benefits of optimizing CoMP scheduling and NOMA clustering jointly with power allocation in the UNC and LNC schemes, we compare our proposed joint strategy with a power allocation approach in which the NOMA clustering and CoMP scheduling are predefined (actually  $\theta$  is predefined) based on the RSS at users considered in [3]. In this line, for LNC, we also need to apply a heuristic approach (as a benchmark) determining  $\mathbf{x}$  before power allocation optimization. Since this scheme is not yet investigated in the literature, we propose a heuristic approach to determine  $\mathbf{x}$  according to the determined  $\theta$  (based on the RSS at users [3]) as follows: First, we note that  $\mathbf{x}$  should satisfy constraint (10). Furthermore, the choice of  $\mathbf{x}$  affects the INI power at users which impacts on the ICI power. In this approach, each CoMP-user selects the local NOMA set which results in the lowest interference power at the user. According to (12), for each user  $k$  over bandwidth  $W_i$ , we set  $x_{i,b,k} = 1$  if

$$b = \arg \min_{b \in \mathcal{C}_{i,k}} \left\{ \sum_{\substack{k' \in \mathcal{K}_i \\ \lambda_{i,k'} > \lambda_{i,k}}} \theta_{i,b,k'} \sum_{b' \in \mathcal{B}_i} \theta_{i,b',k'} p_{i,b',k'} h_{i,b',k} + \sum_{\substack{k' \in \mathcal{K}_i \\ k' \neq k}} (1 - \theta_{i,b,k'}) \sum_{\substack{b' \in \mathcal{B}_i \\ b' \neq b}} \theta_{i,b',k'} p_{i,b',k'} h_{i,b',k} \right\}.$$

The value of  $\mathbf{p}$  is determined based on the equal power allocation strategy. It is noteworthy that the heuristic approaches mentioned above are also used for initializing parameters in our proposed sequential programming algorithms.

We also investigate the impact of number of users, SLAs, and transmit power of FBSs on the performance of SV-CoMP-NOMA. Last but not least, we compare the performance of our proposed locally and globally optimal solutions for the UNC and LNC schemes.



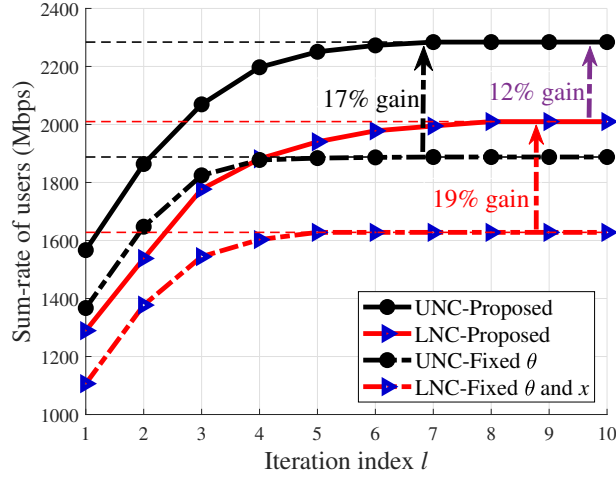
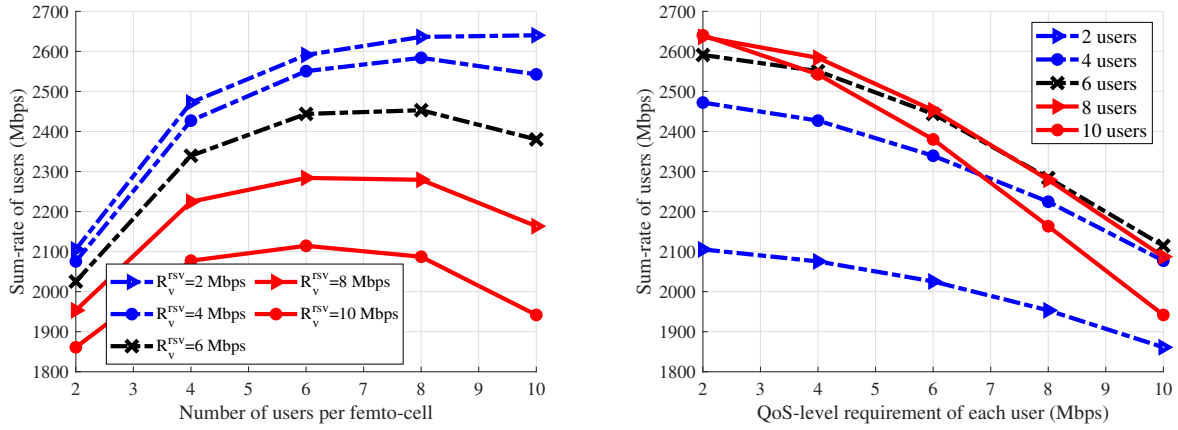


Fig. 7. The SCA convergence of our proposed and benchmark algorithms (fixed  $\theta$  and  $x$ ) in terms of sum-rate of users over iteration index  $l$  for the UNC and LNC schemes.

### C. Convergence Speed

Fig. 7 investigates the convergence speed of our proposed SCA algorithms for the UNC and LNC schemes. As shown, these iterative algorithms converge to stable values in maximum 7 iterations (the dash-lines refer to the upper-bound solution of SCA). Moreover, UNC outperforms LNC in terms of users sum-rate by nearly 12%. This is due to the fact that in LNC, each user  $k$  performs SIC (on each bandwidth  $W_i$ ) to only the signal(s) of users belonging to the selected local NOMA set  $\Phi_{i,b,k}^{\text{Cell}}$  which is a subset of its global NOMA set.

We also compare our proposed joint strategy with the power allocation strategy alone for a predefined user scheduling described in Subsection IV-B. Fig. 7 shows that the joint optimization of power allocation and user scheduling improves users sum-rate by up to 17% compared to the power allocation optimization for the predefined NOMA clustering and CoMP scheduling policies. It is noteworthy that the convergence speed of the power allocation optimization alone for a fixed  $\theta$  and  $x$  would be faster than the joint optimization algorithm, which imposes additional auxiliary variables and constraints due to the series of transformations discussed in



(a) Sum-rate of users vs. number of users per femto-cell for different SLAs. (b) Sum-rate of users vs. SLA of each user for different number of users per femto-cell.

Fig. 8. Impact of SLA and number of users on users sum-rate in the UNC-based SV-CoMP-NOMA system.

Subsection III-A2. However, the gaps between the convergence speed of our proposed algorithm and benchmark are pretty low and negligible compared to the performance gaps.

#### D. Impact of Number of Users and Service Level Agreements

Fig. 8 investigates the impact of number of users on the system performance for different SLAs in the UNC-based SV-CoMP-NOMA system<sup>12</sup>. From Fig. 8(a), it can be observed that for smaller order of number of users, increasing the number of users improves the users sum-rate. This is due to the fact that when the number of users is small enough, the network can efficiently exploit the multi-user diversity. However, when the number of users keeps increasing, the system needs to allocate its resources to a larger number of users with poor channel conditions, due to the SLA constraints in (18b). The performance loss due to the restriction of the flexibility of

<sup>12</sup>Our proposed LNC model is a special case of UNC. Therefore, SLAs have the same impact in both the UNC and LNC schemes. To avoid duplicated presentations, we present the impact of SLAs on only the UNC model.

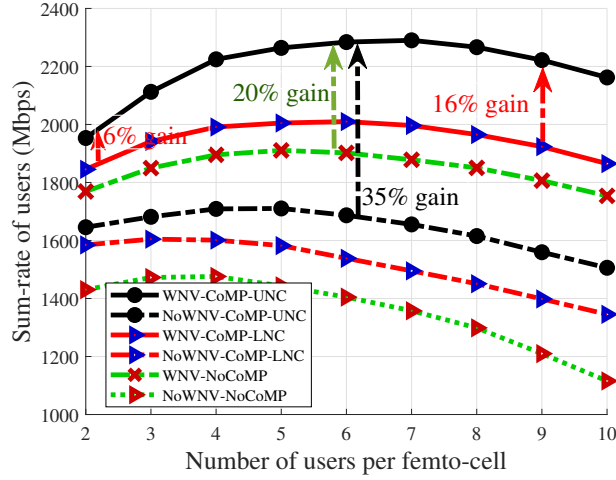


Fig. 9. Sum-rate of users vs. number of users per femto-cell for different schemes with/without CoMP and WNV, when  $R_v^{\text{rsv}} = 8$  Mbps.

resource allocation is dominant compared to the multi-user diversity gain, when the number of users is large enough. As a result, this increment leads to sum-rate degradation shown in Fig. 8(a), specifically when the number of users is large enough. Inversely, in Fig. 8(b), we show the impact of SLA on users sum-rate for different number of users. According to the above discussions, increasing  $R_v^{\text{rsv}}$  degrades the users sum-rate. However, when the number of users is small enough, SLA has not a significant impact on the users sum-rate. Actually, the impact of SLA is more significant for larger number of users.

#### E. Effect of WNV and CoMP on the UNC and LNC Schemes

Fig. 9 shows the impact of the number of users in different scenarios with/without WNV and CoMP in UNC and LNC. As shown, UNC outperforms LNC in terms of sum-rate of users, specifically for the larger number of users. As is mentioned in Subsection II-B2, in the non-CoMP systems (multi-cell NOMA systems without CoMP), since each user is a non-CoMP-user, the global NOMA set of each user is equal to its local NOMA set. Hence, UNC and LNC result

in the same SINR expression, so the same performance in non-CoMP (traditional multi-cell NOMA systems without CoMP) systems. From Fig. 9, it can be observed that applying WNV to multi-infrastructure CoMP-NOMA systems would result in performance gain up to 35%. This significant performance gain is achieved due to the following two unique advantages of WNV: 1) Providing multi-connectivity opportunity for users who are not scheduled for joint transmission of CoMP (e.g., cell-center users); 2) Providing multiple joint transmissions of CoMP from nearby VBSs over orthogonal bands (e.g., cell-edge users). The first advantage has more impact on maximizing users sum-rate, and the second one can improve fairness among users. Besides, applying CoMP to the virtualized multi-infrastructure NOMA systems results in performance gain near to 20%.

#### *F. SIC Complexity of UNC and LNC Schemes*

The SIC complexity at each user is directly proportional to the number of NOMA users decoded and canceled by that user (called order of NOMA cluster) over the shared wireless band. Different metrics could be considered as SIC complexity cost of users. Here, we consider the following two metrics: 1) SIC energy consumption; 2) Complexity of users hardware for decoding and canceling the signals of multiple users in a NOMA cluster. The SIC energy consumption at each user corresponds to the total number of users decoded and canceled by that user. Therefore, we consider the total number of users decoded and canceled by each user as SIC energy consumption of that user. In this paper, we consider a simplified NOMA-layer metric as SIC complexity of users, where the SIC complexity is evaluated by the order of NOMA clusters [19], [20], [22]. The total number of users decoded and canceled by user  $k$  in UNC and LNC can be obtained by  $\sum_{i \in \mathcal{I}} |\Phi_{i,k}|$ , and  $\sum_{i \in \mathcal{I}} \sum_{b \in \mathcal{B}_i} x_{i,b,k} |\Phi_{i,b,k}^{\text{Cell}}|$ , respectively. The complexity of users hardware for performing SIC is directly proportional to the maximum number of users decoded and canceled by that user among orthogonal bands. Therefore, we consider this metric as complexity of users hardware for performing SIC. The maximum number of users decoded and

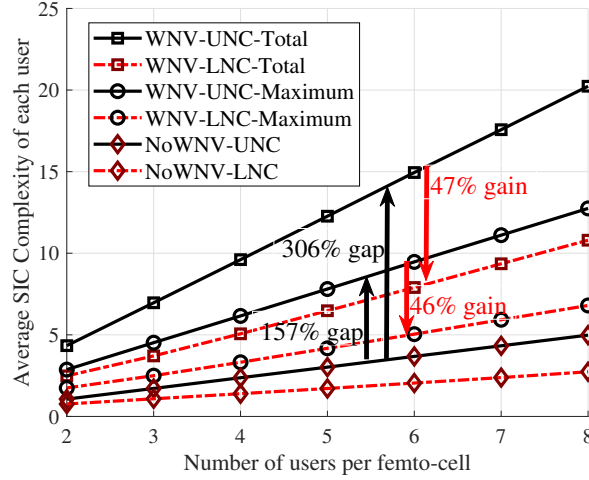


Fig. 10. Average total/maximum number of users decoded and canceled by each NOMA user vs. number of users per femto-cell for the UNC and LNC schemes in CoMP-NOMA systems with/without WNV.

canceled by user  $k$  in UNC and LNC can be obtained by  $\max_{i \in \mathcal{I}} |\Phi_{i,k}|$ , and  $\max_{i \in \mathcal{I}} \sum_{b \in \mathcal{B}_i} x_{i,b,k} |\Phi_{i,b,k}^{\text{Cell}}|$ , respectively. It is noteworthy that for the non-virtualized CoMP-NOMA system, the total and maximum number of users is equal, since each user is assigned to only one InP. In other word, each user forms only one NOMA cluster, and subsequently we have  $\sum_{i \in \mathcal{I}} |\Phi_{i,k}| = \max_{i \in \mathcal{I}} |\Phi_{i,k}|$  in UNC, and  $\sum_{i \in \mathcal{I}} \sum_{b \in \mathcal{B}_i} x_{i,b,k} |\Phi_{i,b,k}^{\text{Cell}}| = \max_{i \in \mathcal{I}} \sum_{b \in \mathcal{B}_i} x_{i,b,k} |\Phi_{i,b,k}^{\text{Cell}}|$  in LNC.

Fig. 10 demonstrates the average complexity cost of performing SIC at each user in two users energy consumption and hardware metrics described in above. As shown, increasing the number of users inherently increases the size of NOMA clusters in single-carrier NOMA systems. In this way, the number of decoded and canceled users increases shown in Fig. 10. Despite the huge potential of WNV in improving users sum-rate in multi-infrastructure CoMP-NOMA systems (shown in Fig. 9), this technology inherently increases the number of NOMA clusters at each user. This is due to breaking of isolation among InPs by WNV resulting in multiple NOMA clusters for each user over orthogonal bandwidths. From Fig. 10, it can be observed that WNV inherently increases the SIC complexity of users by nearly 157% and 306% in LNC and UNC

schemes, respectively. As a result, SIC complexity is more challenging in the SV-CoMP-NOMA system compared to the non-virtualized one, specifically for the larger number of users. More importantly, it can be observed that our proposed LNC has a reduced SIC complexity up to 46% compared to UNC. However, the order of NOMA clusters is still large, due to the single-carrier nature of our system (at each InP). To overcome this issue, the multi-carrier technology can be introduced on SV-CoMP-NOMA, where each sub-band is shared among a limited number of users in a cell [20], [22]. By adopting this technology to LNC, the order of NOMA clusters will be reduced to the NOMA systems without CoMP. However, the multi-carrier systems inherently increase the computational complexity of the central controller on the order of number of sub-bands. The trade-off between the computational complexity of the central controller and the users SIC complexity could be considered as a future work.

#### G. Optimality Gap: Algorithm Performance vs. Computational Complexity

The complexity of our globally optimal solution based on monotonic program is still exponential in the number of optimization variables [42]. Here, we first discuss about the computational complexity of our proposed SCA algorithms. Suppose that we solve the convex approximated form of the UNC problem at SCA iteration  $i$  by using the barrier method with inner Newton's method to achieve an  $\epsilon$ -suboptimal solution. The number of barrier (outer) iterations required to achieve  $\frac{m}{t} = \epsilon$ -suboptimality is exactly  $\Upsilon_i = \lceil \frac{\log(m/(\epsilon t^{(0)}))}{\log \mu} \rceil$ , where  $m$  is the total number of inequality constraints,  $t^{(0)}$  is the initial accuracy parameter for approximating the functions in inequality constraints in standard form, and  $\mu$  is the step size for updating the accuracy parameter  $t$  [47]. The number of inner Newton's iterations depends on  $\mu$  and how good is the initial points at each barrier iteration. [47]. If the SCA algorithm converges to a locally optimal solution after  $\kappa$  iterations, the total number of barrier iterations is  $\sum_{i=1}^{\kappa} \Upsilon_i$ .

Fig. 11 shows sum-rate of users versus maximum power of FBSs in UNC and LNC with our proposed globally and locally optimal solutions. In this simulation, due to the high computational

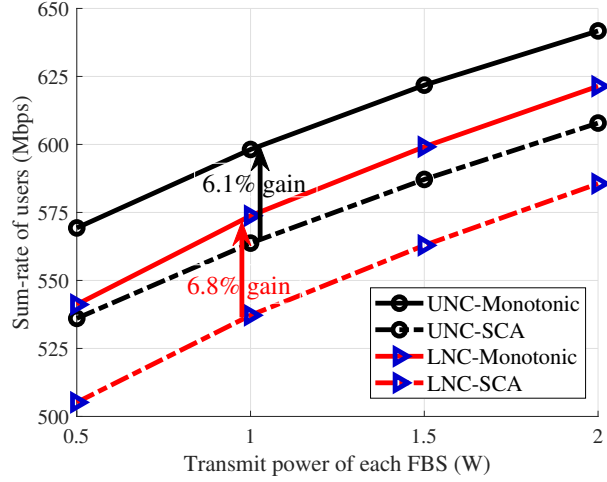


Fig. 11. Sum-rate of users vs. transmit power of each femto-cell for globally and locally optimal algorithms in the UNC and LNC schemes.

complexity of the monotonic optimization, we consider a small scale network [42] with one InP including a single MBS and 2 FBSs in coordinates  $0\angle 0^\circ$ ,  $300\angle 0^\circ$ , and  $300\angle 22.5^\circ$ , respectively. In each femto-cell, we uniformly distribute 2 users [42] (the total number of users is 4) with the same simulation settings as Subsection IV-B. From Fig. 11, it is shown that the optimality gaps are less than 6.8% verifying the efficiency of our proposed locally optimal solutions.

## V. CONCLUDING REMARKS

In this work, we designed a generalized CoMP-NOMA model, where all the cell-edge and cell-center users can benefit from joint transmission of CoMP with specific set of CoMP-BSs. In this model, we devised two NOMA clustering models as UNC and LNC, where UNC performs SIC to all the potential users with lower SIC decoding orders, due to the CoMP-NOMA protocol. Besides, LNC performs SIC to only a subset of potential users which significantly reduces the SIC complexity at users. We proposed one globally and one locally optimal solution for the problem of finding joint power allocation, CoMP scheduling, and NOMA clustering strategies

in the UNC and LNC models. We also investigated the benefits and challenges of applying WNV in multi-infrastructure CoMP-NOMA systems. In simulation results, we observed that our proposed LNC scheme reduces the SIC complexity of users up to 45% compared to UNC. Moreover, it is shown that WNV significantly improves users sum-rate by breaking the isolation among InPs while increasing the number of NOMA clusters at each user.

## APPENDIX A

### CANONICAL TRANSFORMATION OF (18)

To tackle the combinatorial nature of (18),  $\theta$  should be transformed into a continuous variable. Unfortunately, in contrast to the prior works on OMA [48], [49], we cannot relax  $\theta$  to a continuous variable between 0 and 1 by using the time sharing method. Actually, in downlink NOMA systems, we need to determine which part of a frame time is assigned to which user since the superposition coding and SIC (at BSs and users, respectively) are performed according to the set of users receiving signals on the same frequency band at the same time. To overcome this challenge, we transform (18e) into the following equivalent constraint sets as

$$\theta_{i,b,k} \leq \theta_{i,b,k}^2, \quad 0 \leq \theta_{i,b,k} \leq 1. \quad (21)$$

Since the square of each variable in  $(0, 1)$  is smaller than that variable, with (21), the variable  $\theta_{i,b,k}$  can only take zero or one while it has a continuous domain  $[0, 1]$ . By substituting (18e) with (21), the problem (18) is equivalently transformed into a problem with a continuous domain. In contrast to [38], [42], the data rate function  $r_k^{\text{UNC}}$  cannot be directly transformed into the difference of two increasing functions. To tackle this, we first substitute the term  $\left(1 - \min \left\{ \sum_{b \in \mathcal{B}_i} \theta_{i,b,k} \theta_{i,b,k'}, 1 \right\}\right)$  in (4) with a new auxiliary variable  $\alpha_{i,k,k'} \in [0, 1]$  by adding the following constraints

$$\alpha_{i,k,k'} \leq 1 - \theta_{i,b,k} \theta_{i,b,k'}, \quad 0 \leq \alpha_{i,k,k'} \leq 1. \quad (22)$$

$$\alpha_{i,k,k'} \geq 1 - \sum_{b \in \mathcal{B}_i} \theta_{i,b,k} \theta_{i,b,k'}. \quad (23)$$



According to (22) and (23), the SINR of user  $k$  on bandwidth  $W_i$  can be rewritten as

$$\hat{\gamma}_{i,k}^{\text{UNC}} = \frac{s_{i,k}}{I_{i,k}^{\text{UNC,INI}} + \hat{I}_{i,k}^{\text{UNC,ICI}} + \sigma_{i,k}^2}, \quad (24)$$

where  $\hat{I}_{i,k}^{\text{UNC,ICI}} = \sum_{\substack{k' \in \mathcal{K}, \\ k' \neq k}} \alpha_{i,k,k'} \sum_{b \in \mathcal{B}_i} \theta_{i,b,k'} p_{i,b,k'} h_{i,b,k}$ . The spectral efficiency of user  $k$  on bandwidth  $W_i$  is rewritten as  $\hat{r}_{i,k}^{\text{UNC,SE}} = \log_2(1 + \hat{\gamma}_{i,k}^{\text{UNC}})$ , and the data rate of user  $k$  is  $\hat{r}_k^{\text{UNC}} = \sum_{i \in \mathcal{I}} W_i \hat{r}_{i,k}^{\text{UNC,SE}}$ .

Accordingly, (18) is rewritten as

$$\max_{\boldsymbol{\theta}, \mathbf{p}, \boldsymbol{\alpha}} \sum_{v \in \mathcal{V}} \sum_{k \in \mathcal{K}_v} \omega_v \hat{r}_k^{\text{UNC}} \quad (25a)$$

s.t., (18c), (18d), (18f), (21)-(23),

$$\min \left\{ \sum_{b \in \mathcal{B}_i} \theta_{i,b,k} \theta_{i,b,k'}, 1 \right\} \hat{\gamma}_{i,k}^{\text{UNC}} \leq \frac{s_{i,k,j}^{\text{VP}}}{I_{i,k,j}^{\text{UNC,VP}} + (\hat{I}_{i,j}^{\text{UNC,ICI}} + \sigma_{i,j}^2)}, \quad \forall i \in \mathcal{I}, k, j \in \mathcal{K}, \lambda_{i,j} > \lambda_{i,k}, \quad (25b)$$

$$\hat{r}_k^{\text{UNC}} \geq R_v^{\text{RSV}}, \forall v \in \mathcal{V}, k \in \mathcal{K}_v, \quad (25c)$$

Problem (25) exhibits a hidden monotonicity structure. Observe that (25a) can be equivalently rewritten as  $q^+(\boldsymbol{\theta}, \mathbf{p}, \boldsymbol{\alpha}) - q^-(\boldsymbol{\theta}, \mathbf{p}, \boldsymbol{\alpha})$ , wherein  $q^+(\boldsymbol{\theta}, \mathbf{p}, \boldsymbol{\alpha})$  and  $q^-(\boldsymbol{\theta}, \mathbf{p}, \boldsymbol{\alpha})$  are increasing in all optimization variables and given, respectively by

$$q^+(\boldsymbol{\theta}, \mathbf{p}, \boldsymbol{\alpha}) = \sum_{v \in \mathcal{V}} \sum_{k \in \mathcal{K}_v} \omega_v \sum_{i \in \mathcal{I}} W_i \log_2 \left( I_{i,k}^{\text{UNC,INI}} + \hat{I}_{i,k}^{\text{UNC,ICI}} + \sigma_{i,k}^2 + s_{i,k} \right), \quad (26)$$

and

$$q^-(\boldsymbol{\theta}, \mathbf{p}, \boldsymbol{\alpha}) = \sum_{v \in \mathcal{V}} \sum_{k \in \mathcal{K}_v} \omega_v \sum_{i \in \mathcal{I}} W_i \log_2 \left( I_{i,k}^{\text{UNC,INI}} + \hat{I}_{i,k}^{\text{UNC,ICI}} + \sigma_{i,k}^2 \right). \quad (27)$$

Then, we define  $\mathbf{p}_{\max} = \{p_{i,b,k}^{\text{mask}}\}, \forall i, b, k$ ,  $\boldsymbol{\theta}_{\max} = \{\theta_{i,b,k}^{\text{mask}}\}, \forall i, b, k$ , and  $\boldsymbol{\alpha}_{\max} = \{\alpha_{i,k,k'}^{\text{mask}}\}, \forall i, k, k' \neq k$ , where  $p_{i,b,k}^{\text{mask}}$ ,  $\theta_{i,b,k}^{\text{mask}}$ , and  $\alpha_{i,k,k'}^{\text{mask}}$  are the maximum possible values that  $p_{i,b,k}$ ,  $\theta_{i,b,k}$ , and  $\alpha_{i,k,k'}$  can take. Next, we define a new auxiliary variable  $s_0 = q^-(\boldsymbol{\theta}_{\max}, \mathbf{p}_{\max}, \boldsymbol{\alpha}_{\max}) - q^-(\boldsymbol{\theta}, \mathbf{p}, \boldsymbol{\alpha})$ .

Accordingly, (25) can be rewritten as

$$\max_{\boldsymbol{\theta}, \mathbf{p}, \boldsymbol{\alpha}, s_0} q^+(\boldsymbol{\theta}, \mathbf{p}, \boldsymbol{\alpha}) + s_0 \quad (28a)$$

$$\text{s.t. (18c), (18d), (18f), (21)-(23), (25b), (25c),}$$

$$0 \leq s_0 + q^-(\boldsymbol{\theta}, \mathbf{p}, \boldsymbol{\alpha}) \leq q^-(\boldsymbol{\theta}_{\max}, \mathbf{p}_{\max}, \boldsymbol{\alpha}_{\max}), \quad (28b)$$

$$0 \leq s_0 \leq q^-(\boldsymbol{\theta}_{\max}, \mathbf{p}_{\max}, \boldsymbol{\alpha}_{\max}) - q^-(\mathbf{0}_{i,b,k}, \mathbf{0}_{i,b,k}, \mathbf{0}_{i,k,k'}). \quad (28c)$$

Problem (28) is still not a monotonic program, due to constraints (21), (25b), and (25c). Con-

straint (21) can be equivalently rewritten as the following single constraint  $\min_{\substack{i \in \mathcal{I}, b \in \mathcal{B}_i, \\ k \in \mathcal{K}}} [c_{i,b,k}^{1+}(\boldsymbol{\theta}) - c_{i,b,k}^{1-}(\boldsymbol{\theta})] \geq 0$ , where  $c_{i,b,k}^{1+}(\boldsymbol{\theta}) = \theta_{i,b,k}^2$  and  $c_{i,b,k}^{1-}(\boldsymbol{\theta}) = \theta_{i,b,k}$ . The latter constraint is equivalent to

$$\begin{aligned} \min_{\substack{i \in \mathcal{I}, b \in \mathcal{B}_i, \\ k \in \mathcal{K}}} \left[ c_{i,b,k}^{1+}(\boldsymbol{\theta}) - \left( \sum_{i \in \mathcal{I}} \sum_{b \in \mathcal{B}_i} \sum_{k \in \mathcal{K}} c_{i,b,k}^{1-}(\boldsymbol{\theta}) - \sum_{i \in \mathcal{I}} \sum_{b \in \mathcal{B}_i} \sum_{\substack{k' \in \mathcal{K}, \\ k' \neq k}} c_{i,b,k'}^{1-}(\boldsymbol{\theta}) \right) \right] = \\ \underbrace{\min_{\substack{i \in \mathcal{I}, b \in \mathcal{B}_i, \\ k \in \mathcal{K}}} \left[ c_{i,b,k}^{1+}(\boldsymbol{\theta}) + \sum_{i \in \mathcal{I}} \sum_{b \in \mathcal{B}_i} \sum_{\substack{k' \in \mathcal{K}, \\ k' \neq k}} c_{i,b,k'}^{1-}(\boldsymbol{\theta}) \right]}_{c^{1+}(\boldsymbol{\theta})} - \underbrace{\sum_{i \in \mathcal{I}} \sum_{b \in \mathcal{B}_i} \sum_{k \in \mathcal{K}} c_{i,b,k}^{1-}(\boldsymbol{\theta})}_{c^{1-}(\boldsymbol{\theta})} \geq 0, \quad (29) \end{aligned}$$

which is the difference of two increasing functions  $c^{1+}(\boldsymbol{\theta})$  and  $c^{1-}(\boldsymbol{\theta})$ . Similarly, by introducing a new auxiliary variable  $s_1$ , (28) can be rewritten as

$$\max_{\boldsymbol{\theta}, \mathbf{p}, \boldsymbol{\alpha}, s_0, s_1} q^+(\boldsymbol{\theta}, \mathbf{p}, \boldsymbol{\alpha}) + s_0 \quad (30a)$$

$$\text{s.t. (18c), (18d), (18f), (22), (23), (25b), (25c), (28b), (28c),}$$

$$0 \leq s_1 + c^{1-}(\boldsymbol{\theta}) \leq c^{1-}(\boldsymbol{\theta}_{\max}), \quad (30b)$$

$$0 \leq s_1 \leq c^{1-}(\boldsymbol{\theta}_{\max}) - c^{1-}(\mathbf{0}_{i,b,k}), \quad (30c)$$

$$s_1 + c^{1+}(\boldsymbol{\theta}) \geq c^{1-}(\boldsymbol{\theta}_{\max}). \quad (30d)$$

Similar to (21), constraints (25b) and (25c) can be equivalently transformed into the difference of two increasing functions. After adopting this method to (25b) and (25c), the problem (30) can be reformulated as

$$\max_{\boldsymbol{\theta}, \mathbf{p}, \boldsymbol{\alpha}, s_0, s_1, s_2, s_3} q^+(\boldsymbol{\theta}, \mathbf{p}, \boldsymbol{\alpha}) + s_0 \quad (31a)$$

$$\text{s.t. (18c), (18d), (18f), (22), (23), (28b), (28c), (30b)-(30d),}$$

$$0 \leq s_2 + c^{2-}(\boldsymbol{\theta}, \mathbf{p}, \boldsymbol{\alpha}) \leq c^{2-}(\boldsymbol{\theta}_{\max}, \mathbf{p}_{\max}, \boldsymbol{\alpha}_{\max}), \quad (31b)$$

$$0 \leq s_2 \leq c^{2-}(\boldsymbol{\theta}_{\max}, \mathbf{p}_{\max}, \boldsymbol{\alpha}_{\max}) - c^{2-}(\mathbf{0}_{i,b,k}, \mathbf{0}_{i,b,k}, \mathbf{0}_{i,k,k'}), \quad (31c)$$

$$s_2 + c^{2+}(\boldsymbol{\theta}, \mathbf{p}, \boldsymbol{\alpha}) \geq c^{2-}(\boldsymbol{\theta}_{\max}, \mathbf{p}_{\max}, \boldsymbol{\alpha}_{\max}), \quad (31d)$$

$$0 \leq s_3 + c^{3-}(\boldsymbol{\theta}, \mathbf{p}, \boldsymbol{\alpha}) \leq c^{3-}(\boldsymbol{\theta}_{\max}, \mathbf{p}_{\max}, \boldsymbol{\alpha}_{\max}), \quad (31e)$$

$$0 \leq s_3 \leq c^{3-}(\boldsymbol{\theta}_{\max}, \mathbf{p}_{\max}, \boldsymbol{\alpha}_{\max}) - c^{3-}(\mathbf{0}_{i,b,k}, \mathbf{0}_{i,b,k}, \mathbf{0}_{i,k,k'}), \quad (31f)$$

$$s_3 + c^{3+}(\boldsymbol{\theta}, \mathbf{p}, \boldsymbol{\alpha}) \geq c^{3-}(\boldsymbol{\theta}_{\max}, \mathbf{p}_{\max}, \boldsymbol{\alpha}_{\max}), \quad (31g)$$

where  $c^{2+}(\boldsymbol{\theta}, \mathbf{p}, \boldsymbol{\alpha}) = \min_{\substack{i \in \mathcal{I}, k, j \in \mathcal{K} \\ \lambda_{i,j} > \lambda_{i,k}}} \left[ \underbrace{s_{i,k,j} \left( I_{i,k}^{\text{UNC,INI}} + \hat{I}_{i,k}^{\text{UNC,ICI}} + \sigma_{i,k}^2 \right)}_{c_{i,k,j}^{2+}(\boldsymbol{\theta}, \mathbf{p}, \boldsymbol{\alpha})} + \right.$

$$\left. \sum_{i \in \mathcal{I}} \sum_{\substack{k' \in \mathcal{K}, \\ k' \neq j}} \sum_{\substack{k'' \in \mathcal{K} \setminus \{k\}, \\ \lambda_{i,k''} > \lambda_{i,k'}}} s_{i,k''} \min \left\{ \sum_{b \in \mathcal{B}_i} \theta_{i,b,k'} \theta_{i,b,k''}, 1 \right\} \underbrace{\left( I_{i,k',k''}^{\text{UNC,VP}} + \hat{I}_{i,k',k''}^{\text{UNC,ICI}} + \sigma_{i,k''}^2 \right)}_{c_{i,k',k''}^{2-}(\boldsymbol{\theta}, \mathbf{p}, \boldsymbol{\alpha})} \right],$$

$$c^{2-}(\boldsymbol{\theta}, \mathbf{p}, \boldsymbol{\alpha}) = \sum_{i \in \mathcal{I}} \sum_{k' \in \mathcal{K}} \sum_{\substack{k'' \in \mathcal{K}, \\ \lambda_{i,k''} > \lambda_{i,k'}}} c_{i,k',k''}^{2-}(\boldsymbol{\theta}, \mathbf{p}, \boldsymbol{\alpha}),$$

$$c^{3+}(\boldsymbol{\theta}, \mathbf{p}, \boldsymbol{\alpha}) = \min_{k \in \mathcal{K}} \left[ \underbrace{\sum_{i \in \mathcal{I}} W_i \log_2 \left( I_{i,k}^{\text{UNC,INI}} + \hat{I}_{i,k}^{\text{UNC,ICI}} + \sigma_{i,k}^2 + s_{i,k} \right)}_{c_k^{3+}(\boldsymbol{\theta}, \mathbf{p}, \boldsymbol{\alpha})} + \right.$$

$$\left. \sum_{\substack{j \in \mathcal{K} \\ j \neq k}} \sum_{i \in \mathcal{I}} W_i \log_2 \left( I_{i,j}^{\text{UNC,INI}} + \hat{I}_{i,j}^{\text{UNC,ICI}} + \sigma_{i,j}^2 \right) \right], \text{ and } c^{3-}(\boldsymbol{\theta}, \mathbf{p}, \boldsymbol{\alpha}) = \sum_{v \in \mathcal{V}} \sum_{j \in \mathcal{K}_v} c_j^{3-}(\boldsymbol{\theta}, \mathbf{p}, \boldsymbol{\alpha}) + R_v^{\text{RSV}}.$$

$$\underbrace{\sum_{j \in \mathcal{K}} \sum_{i \in \mathcal{I}} W_i \log_2 \left( I_{i,j}^{\text{UNC,INI}} + \hat{I}_{i,j}^{\text{UNC,ICI}} + \sigma_{i,j}^2 \right)}_{c_j^{3-}(\boldsymbol{\theta}, \mathbf{p}, \boldsymbol{\alpha})}$$

In the following, we prove that (31) is a monotonic optimization problem in canonical form. At first, observe that the objective function (31a) is monotonic in  $(\boldsymbol{\theta}, \mathbf{p}, \boldsymbol{\alpha}, s_0, s_1, s_2, s_3)$ . Then, to show that the feasible set of (31) is an intersection of the normal and co-normal sets (according to Definitions 3-5 in [42]), for any  $(\boldsymbol{\theta}, \mathbf{p}, \boldsymbol{\alpha})$  in the feasible set of (31), we have

$$q^-(\mathbf{0}_{i,b,k}, \mathbf{0}_{i,b,k}, \mathbf{0}_{i,k,k'}) \leq q^-(\boldsymbol{\theta}, \mathbf{p}, \boldsymbol{\alpha}), \quad (32)$$

$$c^{1-}(\mathbf{0}_{i,b,k}) \leq c^{1-}(\boldsymbol{\theta}), \quad (33)$$

$$c^{2-}(\mathbf{0}_{i,b,k}, \mathbf{0}_{i,b,k}, \mathbf{0}_{i,k,k'}) \leq c^{2-}(\boldsymbol{\theta}, \mathbf{p}, \boldsymbol{\alpha}), \quad (34)$$

and

$$c^{3-}(\mathbf{0}_{i,b,k}, \mathbf{0}_{i,b,k}, \mathbf{0}_{i,k,k'}) \leq c^{3-}(\boldsymbol{\theta}, \mathbf{p}, \boldsymbol{\alpha}). \quad (35)$$

To this end, the feasible set of (31) can be written as the intersection of the following two sets as

$$\mathcal{S} = \left\{ (\boldsymbol{\theta}, \mathbf{p}, \boldsymbol{\alpha}, s_0, s_1, s_2, s_3) : \boldsymbol{\theta} \preceq \boldsymbol{\theta}_{\max}, \mathbf{p} \preceq \mathbf{p}_{\max}, \boldsymbol{\alpha} \preceq \boldsymbol{\alpha}_{\max}, (18c), (18d), (22), (28b), (28c), \right. \\ \left. (30b), (30c), (31b), (31c), (31e), (31f) \right\}, \quad (36)$$

and

$$\mathcal{S}_c = \left\{ (\boldsymbol{\theta}, \mathbf{p}, \boldsymbol{\alpha}, s_0, s_1, s_2, s_3) : \boldsymbol{\theta} \succeq \mathbf{0}, \mathbf{p} \succeq \mathbf{0}, \boldsymbol{\alpha} \succeq \mathbf{0}, (23), (30d), (31d), (31g) \right\}. \quad (37)$$

All the constraint sets in (36) and (37) are monotonic and continuous (because of employing again (32) and Proposition 2 in [42]), resulting  $\mathcal{S}$  and  $\mathcal{S}_c$  in (36) and (37) are normal and co-normal sets, respectively in the hyper-rectangle given by

$$[0, \boldsymbol{\theta}_{\max}] \times [0, \mathbf{p}_{\max}] \times [0, \boldsymbol{\alpha}_{\max}] \times [0, c^{1-}(\boldsymbol{\theta}_{\max}) - c^{1-}(\mathbf{0}_{i,b,k})] \times [0, c^{2-}(\boldsymbol{\theta}_{\max}, \mathbf{p}_{\max}, \boldsymbol{\alpha}_{\max}) - \\ c^{2-}(\mathbf{0}_{i,b,k}, \mathbf{0}_{i,b,k}, \mathbf{0}_{i,k,k'})] \times [0, c^{3-}(\boldsymbol{\theta}_{\max}, \mathbf{p}_{\max}, \boldsymbol{\alpha}_{\max}) - c^{3-}(\mathbf{0}_{i,b,k}, \mathbf{0}_{i,b,k}, \mathbf{0}_{i,k,k'})] \times \\ [0, q^{-}(\boldsymbol{\theta}_{\max}, \mathbf{p}_{\max}, \boldsymbol{\alpha}_{\max}) - q^{-}(\mathbf{0}_{i,b,k}, \mathbf{0}_{i,b,k}, \mathbf{0}_{i,k,k'})].$$

Thus, (31) fulfills Definition 5 in [42] and the proof is completed.

## APPENDIX B

### EQUIVALENT TRANSFORMATION OF (18)

To tackle the combinatorial nature of (18), we first relax (18e) by using (21) [38]. Then, we replace the term  $\min \left\{ \sum_{b \in \mathcal{B}_i} \theta_{i,b,k} \theta_{i,b,k'}, 1 \right\}$  in (4) with a new auxiliary variable  $\alpha_{i,k,k'} \in [0, 1]$  by adding the following linear constraints:

$$\beta_{i,b,k,k'} \leq \frac{\theta_{i,b,k} + \theta_{i,b,k'}}{2}, \quad 0 \leq \beta_{i,b,k,k'} \leq 1, \quad (38)$$

$$\alpha_{i,k,k'} \leq \sum_{b \in \mathcal{B}_i} \beta_{i,b,k,k'}, \quad (39)$$

$$\alpha_{i,k,k'} \geq \max_{b \in \mathcal{B}_i} \{\theta_{i,b,k} + \theta_{i,b,k'} - 1\}, \quad 0 \leq \alpha_{i,k,k'} \leq 1, \quad (40)$$

in which the binary variable  $\beta_{i,b,k,k'}$  is added to tackle the binary bilinear product  $\theta_{i,b,k}\theta_{i,b,k'}$ .

According to the above transformations, (18) can be rewritten as

$$\max_{\boldsymbol{\theta}, \boldsymbol{p}, \boldsymbol{\alpha}, \boldsymbol{\beta}} \sum_{v \in \mathcal{V}} \sum_{k \in \mathcal{K}_v} \omega_v \hat{r}_k^{\text{UNC}} \quad (41a)$$

s.t. (18c), (18d), (18f), (21), (38)-(40),

$$\alpha_{i,k,j} \frac{S_{i,k}}{\hat{I}_{i,k}^{\text{UNC,INI}} + (\hat{I}_{i,k}^{\text{UNC,ICI}} + \sigma_{i,k}^2)} \leq \frac{S_{i,k,j}^{\text{VP}}}{\hat{I}_{i,k,j}^{\text{UNC,VP}} + (\hat{I}_{i,j}^{\text{UNC,ICI}} + \sigma_{i,j}^2)}, \quad \forall i \in \mathcal{I}, \quad k, j \in \mathcal{K}, \quad \lambda_{i,j} > \lambda_{i,k}, \quad (41b)$$

$$\hat{r}_k^{\text{UNC}} \geq R_v^{\text{rsv}}, \quad \forall v \in \mathcal{V}, \quad k \in \mathcal{K}_v, \quad (41c)$$

where  $\boldsymbol{\alpha} = [\alpha_{i,k,k'}]$ ,  $\boldsymbol{\beta} = [\beta_{i,b,k,k'}]$ ,  $\hat{I}_{i,k}^{\text{UNC,INI}} = \sum_{\substack{k' \in \mathcal{K}, \\ \lambda_{i,k'} > \lambda_{i,k}}} \alpha_{i,k,k'} \sum_{b \in \mathcal{B}_i} \theta_{i,b,k'} p_{i,b,k'} h_{i,b,k}$ ,  $\hat{I}_{i,k}^{\text{UNC,ICI}} = \sum_{\substack{k' \in \mathcal{K}, \\ k' \neq k}} (1 - \alpha_{i,k,k'}) \sum_{b \in \mathcal{B}_i} \theta_{i,b,k'} p_{i,b,k'} h_{i,b,k}$ ,  $\hat{I}_{i,k,j}^{\text{UNC,VP}} = \sum_{\substack{k' \in \mathcal{K}, \\ \lambda_{i,k'} > \lambda_{i,k}}} \alpha_{i,k,k'} \sum_{b \in \mathcal{B}_i} \theta_{i,b,k'} p_{i,b,k'} h_{i,b,j}$ . and  $\hat{\gamma}_{i,k}^{\text{UNC}} = \frac{S_{i,k}}{\hat{I}_{i,k}^{\text{UNC,INI}} + \hat{I}_{i,k}^{\text{UNC,ICI}} + \sigma_{i,k}^2}$ . The spectral efficiency of user  $k$  is obtained by  $\hat{r}_k^{\text{UNC}} = \sum_{i \in \mathcal{I}} W_i \hat{r}_{i,k}^{\text{UNC,SE}}$ , in which  $\hat{r}_{i,k}^{\text{UNC,SE}} = \log_2(1 + \hat{\gamma}_{i,k}^{\text{UNC}})$ . Problem (41) cannot be directly solved by the SCA algorithm yet, due to the multiplications of  $\boldsymbol{\theta}$ ,  $\boldsymbol{p}$ , and  $\boldsymbol{\alpha}$  (in the SINR function  $\hat{\gamma}_{i,k}^{\text{UNC}}$ ), and fractional constraint (41b). In this regard, we first substitute the product term  $\theta_{i,b,k} p_{i,b,k}$  with  $\tilde{p}_{i,b,k}$  by imposing the following constraints [38]:

$$\tilde{p}_{i,b,k} \leq \theta_{i,b,k} P_{i,b}^{\max}, \quad \tilde{p}_{i,b,k} \leq p_{i,b,k}, \quad \tilde{p}_{i,b,k} \geq p_{i,b,k} - (1 - \theta_{i,b,k}) P_{i,b}^{\max}. \quad (42)$$

Since  $\alpha_{i,k,k'} = \min \left\{ \sum_{b \in \mathcal{B}_i} \theta_{i,b,k} \theta_{i,b,k'}, 1 \right\}$ , we have  $\alpha_{i,k,k'} = \alpha_{i,k',k}$ . After these transformations, we substitute  $\alpha_{i,k,k'} \tilde{p}_{i,b,k}$  and  $(1 - \alpha_{i,k,k'}) \tilde{p}_{i,b,k}$  with  $q_{i,b,k,k'}$  and  $\bar{q}_{i,b,k,k'}$ , respectively by adding the following constraint sets, respectively as

$$q_{i,b,k,k'} \leq \alpha_{i,k,k'} P_{i,b}^{\max}, \quad q_{i,b,k,k'} \leq \tilde{p}_{i,b,k}, \quad q_{i,b,k,k'} \geq \tilde{p}_{i,b,k} - (1 - \alpha_{i,k,k'}) P_{i,b}^{\max}, \quad (43)$$

and

$$\bar{q}_{i,b,k,k'} \leq (1 - \alpha_{i,k,k'}) P_{i,b}^{\max}, \quad \bar{q}_{i,b,k,k'} \leq \tilde{p}_{i,b,k}, \quad \bar{q}_{i,b,k,k'} \geq \tilde{p}_{i,b,k} - (1 - (1 - \alpha_{i,k,k'})) P_{i,b}^{\max}. \quad (44)$$

According to the above transformations, we have  $\tilde{I}_{i,k}^{\text{UNC,INI}} = \sum_{\substack{k' \in \mathcal{K}, \\ \lambda_{i,k'} > \lambda_{i,k}}} \sum_{b \in \mathcal{B}_i} q_{i,b,k',k} h_{i,b,k}$ ,  $\tilde{I}_{i,k}^{\text{UNC,ICI}} = \sum_{\substack{k' \in \mathcal{K}, \\ \lambda_{i,k'} > \lambda_{i,k}}} \sum_{b \in \mathcal{B}_i} \tilde{p}_{i,b,k} h_{i,b,k}$ , and  $\tilde{\gamma}_{i,k}^{\text{UNC}} = \frac{\sum_{b \in \mathcal{B}_i} \tilde{p}_{i,b,k} h_{i,b,k}}{\tilde{I}_{i,k}^{\text{UNC,INI}} + \tilde{I}_{i,k}^{\text{UNC,ICI}} + \sigma_{i,k}^2}$ . Moreover, the SIC constraint (41b) can be rewritten as

$$\frac{\sum_{b \in \mathcal{B}_i} q_{i,b,k,j} h_{i,b,k}}{\tilde{I}_{i,k}^{\text{UNC,INI}} + (\tilde{I}_{i,k}^{\text{UNC,ICI}} + \sigma_{i,k}^2)} \leq \frac{\sum_{b \in \mathcal{B}_i} \tilde{p}_{i,b,k} h_{i,b,j}}{\tilde{I}_{i,k,j}^{\text{UNC,VP}} + (\tilde{I}_{i,j}^{\text{UNC,ICI}} + \sigma_{i,j}^2)}, \quad \forall i \in \mathcal{I}, k, j \in \mathcal{K}, \lambda_{i,j} > \lambda_{i,k}, \quad (45)$$

Thus, (41) can be transformed into the following problem as

$$\max_{\boldsymbol{\vartheta}} \sum_{v \in \mathcal{V}} \sum_{k \in \mathcal{K}_v} \omega_v \tilde{r}_k^{\text{UNC}} \quad (46a)$$

$$\text{s.t. (18c), (18d), (18f), (21), (38)-(40), (42)-(44), (45),}$$

$$\tilde{r}_k^{\text{UNC}} \geq R_v^{\text{rsv}}, \forall v \in \mathcal{V}, k \in \mathcal{K}_v, \quad (46b)$$

where  $\tilde{r}_k^{\text{UNC}} = \sum_{i \in \mathcal{I}} W_i \tilde{r}_{i,k}^{\text{UNC,SE}}$  in which  $\tilde{r}_{i,k}^{\text{UNC,SE}} = \log_2(1 + \tilde{\gamma}_{i,k}^{\text{UNC}})$ . Moreover, to ease of convenience, we denote  $\mathbf{q} = [q_{i,b,k,k'}]$ ,  $\bar{\mathbf{q}} = [\bar{q}_{i,b,k,k'}]$ ,  $\tilde{\mathbf{p}} = [\tilde{p}_{i,b,k}]$ , and  $\boldsymbol{\vartheta} = [\boldsymbol{\theta}, \mathbf{p}, \boldsymbol{\alpha}, \boldsymbol{\beta}, \mathbf{q}, \bar{\mathbf{q}}, \tilde{\mathbf{p}}]$ . Problem (46) is still nonconvex, due to the nonconcavity of the objective function in (46a), and nonconvexity of constraints (21), (45), and (46b). To handle (21), we use the penalty factor approach, where for a sufficiently large constant  $\eta \gg 1$ , (46) can be equivalently transformed into the following problem [38]:

$$\max_{\boldsymbol{\vartheta}} \sum_{v \in \mathcal{V}} \sum_{k \in \mathcal{K}_v} \omega_v \tilde{r}_k^{\text{UNC}} - \eta \left( \sum_{i \in \mathcal{I}} \sum_{b \in \mathcal{B}_i} \sum_{k \in \mathcal{K}} \theta_{i,b,k} - \theta_{i,b,k}^2 \right) \quad (47a)$$

$$\text{s.t. (18c), (18d), (18f), (38)-(40), (42)-(44), (45), (46b),}$$

$$0 \leq \theta_{i,b,k} \leq 1. \quad (47b)$$

In fact,  $\eta$  acts as a penalty factor for the objective function to penalize the cost term  $(\theta_{i,b,k} - \theta_{i,b,k}^2)$  in (47a). The proof of this theorem is similar to the proof presented in the appendix of [38]. The

resulting problem (47) is still nonconvex, due to the nonconcavity of the SINR function in (45), (46b), and (47a), and also the term  $\theta_{i,b,k}^2$  in (47a). In contrast to prior works [35], [38], [40], [45], we cannot directly apply the SCA algorithm with DC programming to solve (47), since (45) cannot be transformed into a linear constraint, due to the weighted sum of signal powers in the numerator of the SINR functions in (45). To tackle this, we first transform (45) into the difference of two concave functions as

$$\begin{aligned} & \log_2 \left( \sum_{b \in \mathcal{B}_i} \tilde{p}_{i,b,k} h_{i,b,j} \right) + \log_2 \left( \tilde{I}_{i,k}^{\text{UNC,INI}} + (\tilde{I}_{i,k}^{\text{UNC,ICI}} + \sigma_{i,k}^2) \right) - \log_2 \left( \sum_{b \in \mathcal{B}_i} q_{i,b,k,j} h_{i,b,k} \right) \\ & - \log_2 \left( \tilde{I}_{i,k,j}^{\text{UNC,VP}} + (\tilde{I}_{i,j}^{\text{UNC,ICI}} + \sigma_{i,j}^2) \right) \geq 0, \quad \forall i \in \mathcal{I}, k, j \in \mathcal{K}, \lambda_{i,j} > \lambda_{i,k}. \end{aligned} \quad (48)$$

Problem (47) can thus be rewritten as

$$\begin{aligned} & \max_{\boldsymbol{\vartheta}} \quad \sum_{v \in \mathcal{V}} \sum_{k \in \mathcal{K}_v} \omega_v \tilde{r}_k^{\text{UNC}} - \eta \left( \sum_{i \in \mathcal{I}} \sum_{b \in \mathcal{B}_i} \sum_{k \in \mathcal{K}} \theta_{i,b,k} - \theta_{i,b,k}^2 \right) \\ & \text{s.t. (18c), (18d), (18f), (38)-(40), (42)-(44), (46b), (47b), (48).} \end{aligned} \quad (49a)$$

The equivalent transformed problem (49) can be solved by using the SCA algorithm with DC programming resulting in locally optimal solution of the original problem (18).

## APPENDIX C

### SCA WITH DC PROGRAMMING FOR SOLVING (49)

To tackle the nonconcavity of the rate function in (49a) and (46b), we first define  $\tilde{r}_{i,k}^{\text{UNC,SE}}(\mathbf{q}, \bar{\mathbf{q}}, \tilde{\mathbf{p}})$  as the difference of two concave functions as  $\tilde{r}_{i,k}^{\text{UNC,SE}}(\mathbf{q}, \bar{\mathbf{q}}, \tilde{\mathbf{p}}) = f_{i,k}^{\text{UNC}}(\mathbf{q}, \bar{\mathbf{q}}, \tilde{\mathbf{p}}) - g_{i,k}^{\text{UNC}}(\mathbf{q}, \bar{\mathbf{q}})$ , where

$$f_{i,k}^{\text{UNC}}(\mathbf{q}, \bar{\mathbf{q}}, \tilde{\mathbf{p}}) = \log_2 \left( \tilde{I}_{i,k}^{\text{UNC,INI}} + \tilde{I}_{i,k}^{\text{UNC,ICI}} + \sigma_{i,k}^2 + \sum_{b \in \mathcal{B}_i} \tilde{p}_{i,b,k} h_{i,b,k} \right), \quad (50)$$

and

$$g_{i,k}^{\text{UNC}}(\mathbf{q}, \bar{\mathbf{q}}) = \log_2 \left( \tilde{I}_{i,k}^{\text{UNC,INI}} + \tilde{I}_{i,k}^{\text{UNC,ICI}} + \sigma_{i,k}^2 \right). \quad (51)$$

Note that  $\tilde{r}_{i,k}^{\text{UNC,SE}}$  is concave with respect to  $\tilde{\mathbf{p}}$ . Then, at each iteration  $l$ , the term  $g_{i,k}^{\text{UNC}}(\mathbf{q}^{(l)}, \bar{\mathbf{q}}^{(l)})$  is approximated to its first order Taylor series approximation around  $(\mathbf{q}^{(l-1)}, \bar{\mathbf{q}}^{(l-1)})$  as

$$g_{i,k}^{\text{UNC}}(\mathbf{q}^{(l)}, \bar{\mathbf{q}}^{(l)}) \approx g_{i,k}^{\text{UNC}}(\mathbf{q}^{(l-1)}, \bar{\mathbf{q}}^{(l-1)}) + \nabla_{\mathbf{q}} g_{i,k}^{\text{UNC}}(\mathbf{q}^{(l-1)}, \bar{\mathbf{q}}^{(l-1)}) (\mathbf{q}^{(l)} - \mathbf{q}^{(l-1)}) + \\ \nabla_{\bar{\mathbf{q}}} g_{i,k}^{\text{UNC}}(\mathbf{q}^{(l-1)}, \bar{\mathbf{q}}^{(l-1)}) (\bar{\mathbf{q}}^{(l)} - \bar{\mathbf{q}}^{(l-1)}), \quad (52)$$

where the gradient functions  $\nabla_{\mathbf{q}} g_{i,k}^{\text{UNC}}(\mathbf{q}, \bar{\mathbf{q}})$  and  $\nabla_{\bar{\mathbf{q}}} g_{i,k}^{\text{UNC}}(\mathbf{q}, \bar{\mathbf{q}})$  are defined, respectively as follows:

$$\nabla_{\mathbf{q}} g_{i,k}^{\text{UNC}}(\mathbf{q}, \bar{\mathbf{q}}) = \begin{cases} \frac{h_{i,b,k}}{(\ln 2)(\tilde{I}_{i,k}^{\text{UNC,INI}} + \tilde{I}_{i,k}^{\text{UNC,ICI}} + \sigma_{i,k}^2)}, & \forall \lambda_{i,k'} > \lambda_{i,k}, b \in \mathcal{B}_i; \\ 0, & \text{otherwise,} \end{cases} \quad (53)$$

$$\nabla_{\bar{\mathbf{q}}} g_{i,k}^{\text{UNC}}(\mathbf{q}, \bar{\mathbf{q}}) = \begin{cases} \frac{h_{i,b,k}}{(\ln 2)(\tilde{I}_{i,k}^{\text{UNC,INI}} + \tilde{I}_{i,k}^{\text{UNC,ICI}} + \sigma_{i,k}^2)}, & \forall k' \in \mathcal{K} \setminus \{k\}, b \in \mathcal{B}_i; \\ 0, & \text{otherwise.} \end{cases} \quad (54)$$

Therefore, at each iteration  $l$ ,  $\tilde{r}_{i,k}^{\text{UNC,SE}}(\mathbf{q}^{(l)}, \bar{\mathbf{q}}^{(l)}, \tilde{\mathbf{p}}^{(l)})$  is approximated by

$$\hat{r}_{i,k}^{\text{UNC,SE}}(\mathbf{q}^{(l)}, \bar{\mathbf{q}}^{(l)}, \tilde{\mathbf{p}}^{(l)}) \approx f_{i,k}^{\text{UNC}}(\mathbf{q}^{(l)}, \bar{\mathbf{q}}^{(l)}, \tilde{\mathbf{p}}^{(l)}) - g_{i,k}^{\text{UNC}}(\mathbf{q}^{(l-1)}, \bar{\mathbf{q}}^{(l-1)}) - \nabla_{\mathbf{q}} g_{i,k}^{\text{UNC}}(\mathbf{q}^{(l-1)}, \bar{\mathbf{q}}^{(l-1)}) \\ (\mathbf{q}^{(l)} - \mathbf{q}^{(l-1)}) - \nabla_{\bar{\mathbf{q}}} g_{i,k}^{\text{UNC}}(\mathbf{q}^{(l-1)}, \bar{\mathbf{q}}^{(l-1)}) (\bar{\mathbf{q}}^{(l)} - \bar{\mathbf{q}}^{(l-1)}). \quad (55)$$

Similarly, to handle the nonconvexity of (48), at each iteration  $l$ , we approximate  $T_{i,b,k,j}^1(\mathbf{q}, \bar{\mathbf{q}}) = \log_2 \left( \sum_{b \in \mathcal{B}_i} q_{i,b,k,j} h_{i,b,k} \right) + \log_2 \left( \tilde{I}_{i,k,j}^{\text{UNC,VP}} + (\tilde{I}_{i,j}^{\text{UNC,ICI}} + \sigma_{i,j}^2) \right)$  to an affine function as follows:

$$\hat{T}_{i,b,k,j}^1(\mathbf{q}^{(l)}, \bar{\mathbf{q}}^{(l)}) \approx T_{i,b,k,j}^1(\mathbf{q}^{(l-1)}, \bar{\mathbf{q}}^{(l-1)}) + \nabla_{\mathbf{q}} T_{i,b,k,j}^1(\mathbf{q}^{(l-1)}, \bar{\mathbf{q}}^{(l-1)}) (\mathbf{q}^{(l)} - \mathbf{q}^{(l-1)}) + \\ \nabla_{\bar{\mathbf{q}}} T_{i,b,k,j}^1(\mathbf{q}^{(l-1)}, \bar{\mathbf{q}}^{(l-1)}) (\bar{\mathbf{q}}^{(l)} - \bar{\mathbf{q}}^{(l-1)}), \quad (56)$$

in which

$$\nabla_{\mathbf{q}} T_{i,b,k,j}^1(\mathbf{q}, \bar{\mathbf{q}}) = \begin{cases} \frac{h_{i,b,k}}{(\ln 2) \left( \sum_{b \in \mathcal{B}_i} q_{i,b,k,j} h_{i,b,k} \right)} + \frac{h_{i,b,j}}{(\ln 2)(\tilde{I}_{i,k,j}^{\text{UNC,VP}} + (\tilde{I}_{i,j}^{\text{UNC,ICI}} + \sigma_{i,j}^2))}, & \forall \lambda_{i,j} > \lambda_{i,k}, b \in \mathcal{B}_i; \\ 0, & \text{otherwise,} \end{cases} \quad (57)$$

and

$$\nabla_{\bar{\mathbf{q}}} T_{i,b,k',k}^1(\mathbf{q}, \bar{\mathbf{q}}) = \begin{cases} \frac{h_{i,b,j}}{(\ln 2)(\tilde{I}_{i,k,j}^{\text{UNC,VP}} + (\tilde{I}_{i,j}^{\text{UNC,ICI}} + \sigma_{i,j}^2))}, & \forall \lambda_{i,j} > \lambda_{i,k}, b \in \mathcal{B}_i; \\ 0, & \text{otherwise.} \end{cases} \quad (58)$$



At each iteration  $l$ , the nonconcave term  $T_{i,b,k}^2 = \theta_{i,b,k}^2$  in (49a) is approximated to its first order Taylor series as

$$\hat{T}_{i,b,k}^2(\boldsymbol{\theta}^{(l)}) \approx T_{i,b,k}^2(\boldsymbol{\theta}^{(l-1)}) + \nabla_{\boldsymbol{\theta}} T_{i,b,k}^2(\boldsymbol{\theta}^{(l-1)}) (\boldsymbol{\theta}^{(l)} - \boldsymbol{\theta}^{(l-1)}), \quad (59)$$

where  $\nabla_{\boldsymbol{\theta}} T_{i,b,k}^2 = 2\theta_{i,b,k}$ . According to (55), (56), and (59), the convex approximated problem of (49) is given by

$$\max_{\boldsymbol{\vartheta}} \sum_{v \in \mathcal{V}} \sum_{k \in \mathcal{K}_v} \omega_v \sum_{i \in \mathcal{I}} W_i \hat{r}_{i,k}^{\text{UNC,SE}} - \eta \left( \sum_{i \in \mathcal{I}} \sum_{b \in \mathcal{B}_i} \sum_{k \in \mathcal{K}} \theta_{i,b,k} - \hat{T}_{i,b,k}^2 \right) \quad (60a)$$

s.t. (18c), (18d), (18f), (38)-(40), (42)-(44), (47b),

$$\sum_{i \in \mathcal{I}} \hat{r}_{i,k}^{\text{UNC,SE}} \geq R_v^{\text{rsv}}, \forall v \in \mathcal{V}, k \in \mathcal{K}_v, \quad (60b)$$

$$\log_2 \left( \sum_{b \in \mathcal{B}_i} \tilde{p}_{i,b,k} h_{i,b,j} \right) + \log_2 \left( \tilde{I}_{i,k}^{\text{UNC,INI}} + (\tilde{I}_{i,k}^{\text{UNC,ICI}} + \sigma_{i,k}^2) \right) - \hat{T}_{i,b,k,j}^1(\mathbf{q}^{(l)}, \bar{\mathbf{q}}^{(l)}) \geq 0,$$

$$\forall i \in \mathcal{I}, k, j \in \mathcal{K}, \lambda_{i,j} > \lambda_{i,k}. \quad (60c)$$

At each iteration  $l$ , the convex optimization problem (60) can be solved by using the standard convex optimization solvers such as Lagrange dual method, interior point methods, or standard optimization software CVX [35], [38], [40], [45].

## APPENDIX D

### CONVERGENCE OF THE PROPOSED SCA ALGORITHM FOR SOLVING (49)

In order to prove that the proposed SCA algorithm converges to a locally optimal solution, we first note that the gradients of  $g_{i,k}^{\text{UNC}}(\mathbf{q}, \bar{\mathbf{q}})$ ,  $\hat{T}_{i,b,k',k}^1(\mathbf{q}^{(l)}, \bar{\mathbf{q}}^{(l)})$ , and  $\hat{T}_{i,b,k}^2(\boldsymbol{\theta}^{(l)})$  are indeed their supergradients meaning that at each iteration  $l$ , for any feasible point  $\boldsymbol{\vartheta}^{(l)}$ , we have

$$g_{i,k}^{\text{UNC}}(\mathbf{q}^{(l)}, \bar{\mathbf{q}}^{(l)}) \leq g_{i,k}^{\text{UNC}}(\mathbf{q}^{(l-1)}, \bar{\mathbf{q}}^{(l-1)}) + \nabla_{\mathbf{q}} g_{i,k}^{\text{UNC}}(\mathbf{q}^{(l-1)}, \bar{\mathbf{q}}^{(l-1)}) (\mathbf{q}^{(l)} - \mathbf{q}^{(l-1)}) + \nabla_{\bar{\mathbf{q}}} g_{i,k}^{\text{UNC}}(\mathbf{q}^{(l-1)}, \bar{\mathbf{q}}^{(l-1)}) (\bar{\mathbf{q}}^{(l)} - \bar{\mathbf{q}}^{(l-1)}), \quad (61)$$

$$\begin{aligned} \hat{T}_{i,b,k',k}^1(\mathbf{q}^{(l)}, \bar{\mathbf{q}}^{(l)}) &\leq T_{i,b,k',k}^1(\mathbf{q}^{(l-1)}, \bar{\mathbf{q}}^{(l-1)}) + \nabla_{\mathbf{q}} T_{i,b,k',k}^1(\mathbf{q}^{(l-1)}, \bar{\mathbf{q}}^{(l-1)}) (\mathbf{q}^{(l)} - \mathbf{q}^{(l-1)}) + \\ &\quad \nabla_{\bar{\mathbf{q}}} T_{i,b,k',k}^1(\mathbf{q}^{(l-1)}, \bar{\mathbf{q}}^{(l-1)}) (\bar{\mathbf{q}}^{(l)} - \bar{\mathbf{q}}^{(l-1)}), \end{aligned} \quad (62)$$

and

$$\hat{T}_{i,b,k}^2(\boldsymbol{\theta}^{(l)}) \leq T_{i,b,k}^2(\boldsymbol{\theta}^{(l-1)}) + \nabla_{\boldsymbol{\theta}} T_{i,b,k}^2(\boldsymbol{\theta}^{(l-1)}) (\boldsymbol{\theta}^{(l)} - \boldsymbol{\theta}^{(l-1)}). \quad (63)$$

According to (61)-(63), it can be easily shown that the optimal solution of (60) remains in the feasible region of (49) which is equivalent to (18). Moreover, according to (61) and (63), for any optimal solution  $(\boldsymbol{\theta}^{*(l)}, \mathbf{q}^{*(l)}, \bar{\mathbf{q}}^{*(l)}, \tilde{\mathbf{p}}^{*(l)})$ , it can be concluded that at each iteration  $l$ , the following inequality holds:

$$\begin{aligned} \sum_{v \in \mathcal{V}} \sum_{k \in \mathcal{K}_v} \omega_v \sum_{i \in \mathcal{I}} W_i \tilde{r}_{i,k}^{\text{UNC,SE}}(\mathbf{q}^{*(l)}, \bar{\mathbf{q}}^{*(l)}, \tilde{\mathbf{p}}^{*(l)}) - \eta \left( \sum_{b \in \mathcal{B}_i} \sum_{k \in \mathcal{K}} \theta_{i,b,k}^{*(l)} - T_{i,b,k}^2(\boldsymbol{\theta}^{*(l)}) \right) \geq \\ \sum_{v \in \mathcal{V}} \sum_{k \in \mathcal{K}_v} \omega_v \sum_{i \in \mathcal{I}} W_i \hat{r}_{i,k}^{\text{UNC,SE}}(\mathbf{q}^{*(l)}, \bar{\mathbf{q}}^{*(l)}, \tilde{\mathbf{p}}^{*(l)}) - \eta \left( \sum_{b \in \mathcal{B}_i} \sum_{k \in \mathcal{K}} \theta_{i,b,k}^{*(l)} - \hat{T}_{i,b,k}^2(\boldsymbol{\theta}^{*(l)}) \right). \end{aligned} \quad (64)$$

According to the fact that at each iteration  $l$ ,  $\boldsymbol{\vartheta}^{*(l)}$  is the globally optimal solution of the convex problem (60) which is in the feasible region of (49), it can be concluded that

$$\begin{aligned} \sum_{v \in \mathcal{V}} \sum_{k \in \mathcal{K}_v} \omega_v \sum_{i \in \mathcal{I}} W_i \hat{r}_{i,k}^{\text{UNC,SE}}(\mathbf{q}^{*(l)}, \bar{\mathbf{q}}^{*(l)}, \tilde{\mathbf{p}}^{*(l)}) - \eta \left( \sum_{b \in \mathcal{B}_i} \sum_{k \in \mathcal{K}} \theta_{i,b,k}^{*(l)} - \hat{T}_{i,b,k}^2(\boldsymbol{\theta}^{*(l)}) \right) \\ = \max_{\boldsymbol{\vartheta}} \sum_{v \in \mathcal{V}} \sum_{k \in \mathcal{K}_v} \omega_v \sum_{i \in \mathcal{I}} W_i \hat{r}_{i,k}^{\text{UNC,SE}}(\mathbf{q}^{(l)}, \bar{\mathbf{q}}^{(l)}, \tilde{\mathbf{p}}^{(l)}) - \eta \left( \sum_{b \in \mathcal{B}_i} \sum_{k \in \mathcal{K}} \theta_{i,b,k}^{(l)} - \hat{T}_{i,b,k}^2(\boldsymbol{\theta}^{(l)}) \right) \\ \geq \sum_{v \in \mathcal{V}} \sum_{k \in \mathcal{K}_v} \omega_v \sum_{i \in \mathcal{I}} W_i \hat{r}_{i,k}^{\text{UNC,SE}}(\mathbf{q}^{(l-1)}, \bar{\mathbf{q}}^{(l-1)}, \tilde{\mathbf{p}}^{(l-1)}) - \eta \left( \sum_{b \in \mathcal{B}_i} \sum_{k \in \mathcal{K}} \theta_{i,b,k}^{(l-1)} - \hat{T}_{i,b,k}^2(\boldsymbol{\theta}^{(l-1)}) \right) \\ = \sum_{v \in \mathcal{V}} \sum_{k \in \mathcal{K}_v} \omega_v \sum_{i \in \mathcal{I}} W_i \tilde{r}_{i,k}^{\text{UNC,SE}}(\mathbf{q}^{(l-1)}, \bar{\mathbf{q}}^{(l-1)}, \tilde{\mathbf{p}}^{(l-1)}) - \eta \left( \sum_{b \in \mathcal{B}_i} W_i \sum_{k \in \mathcal{K}} \theta_{i,b,k}^{(l-1)} - T_{i,b,k}^2(\boldsymbol{\theta}^{(l-1)}) \right). \end{aligned} \quad (65)$$

According to (64) and (65), it can be derived that after each SCA iteration, the objective function (49a) is improved (increased) or remains constant. Therefore, the proposed SCA algorithm with DC programming converges to a locally optimal solution and the proof is completed.

## APPENDIX E

## CANONICAL TRANSFORMATION OF (19)

In order to transform (19) into a monotonic-based optimization problem in canonical form, we first relax  $\theta$  and  $x$  by using the relaxation approach in (21). Then, we substitute the term  $(1 - \theta_{i,b,k})$  in  $I_{i,k}^{\text{LNC,ICI}}$  in (12) with  $\bar{\theta}_{i,b,k}$  by adding the following constraint as

$$\bar{\theta}_{i,b,k} \geq 1 - \theta_{i,b,k}, \quad 0 \leq \bar{\theta}_{i,b,k} \leq 1. \quad (66)$$

In this regard,  $I_{i,k}^{\text{LNC,ICI}}$  is substituted with  $\hat{I}_{i,k}^{\text{LNC,ICI}} = \sum_{b \in \mathcal{B}_i} x_{i,b,k} \sum_{\substack{k' \in \mathcal{K}, \\ k' \neq k}} \bar{\theta}_{i,b,k'} \sum_{\substack{b' \in \mathcal{B}_i, \\ b' \neq b}} \theta_{i,b',k'} p_{i,b',k'} h_{i,b',k}$ .

Therefore, (19) can be rewritten as

$$\max_{\theta, x, p, \bar{\theta}} \sum_{v \in \mathcal{V}} \sum_{k \in \mathcal{K}_v} \omega_v \hat{r}_k^{\text{LNC}} \quad (67a)$$

s.t. (9), (10), (18c), (18d), (18f), (21),

$$x_{i,b,k} \theta_{i,b,j} \frac{s_{i,k}}{I_{i,k}^{\text{LNC,INI}} + (\hat{I}_{i,k}^{\text{LNC,ICI}} + \sigma_{i,k}^2)} \leq \frac{s_{i,k,j}^{\text{VP}}}{I_{i,k,j}^{\text{LNC,VP}} + (\hat{I}_{i,j}^{\text{LNC,ICI}} + \sigma_{i,j}^2)}, \quad \forall i \in \mathcal{I}, \quad b \in \mathcal{B}_i, \quad (67b)$$

$$k, k' \in \mathcal{K}, \quad \lambda_{i,k} > \lambda_{i,k'}, \quad (67b)$$

$$\hat{r}_k^{\text{LNC}} \geq R_v^{\text{TSV}}, \quad \forall v \in \mathcal{V}, k \in \mathcal{K}_v, \quad (67c)$$

$$x_{i,b,k} \leq x_{i,b,k}^2, \quad 0 \leq x_{i,b,k} \leq 1, \quad (67d)$$

where  $\hat{r}_k^{\text{LNC}} = \sum_{i \in \mathcal{I}} W_i \log_2 \left( 1 + \frac{s_{i,k}}{I_{i,k}^{\text{LNC,INI}} + \hat{I}_{i,k}^{\text{LNC,ICI}} + \sigma_{i,k}^2} \right)$ , and  $\bar{\theta} = [\bar{\theta}_{i,b,k}]$ . Problem (67) is not yet a monotonic optimization problem in canonical form, because of the objective function (67a) and constraints (21), (67b)-(67d). To tackle the non-monotonicity of (21) and (67d), we apply a similar transformation method that is used in (29) and constraints (30b)-(30d). Moreover, for the non-monotonic constraints (67b) and (67c), we apply a similar method to the approach used in constraint sets (31b)-(31d) and (31e)-(31g), respectively. In addition, for the non-monotonic objective function (67a), we apply a similar method that is used in (26)-(28). After adopting the above steps, the resulting monotonic problem would be canonical which can be optimally

solved by using the poly block or branch-reduce-and-bound algorithms [42]. In order to avoid duplicated discussions, the canonical form of (67) is not mathematically formulated here.

## REFERENCES

- [1] R. Irmer, H. Droste, P. Marsch, M. Grieger, G. Fettweis, S. Brueck, H. Mayer, L. Thiele, and V. Jungnickel, "Coordinated multipoint: Concepts, performance, and field trial results," *IEEE Communications Magazine*, vol. 49, no. 2, pp. 102–111, Feb. 2011.
- [2] M. S. Ali, E. Hossain, and D. I. Kim, "Coordinated multipoint transmission in downlink multi-cell NOMA systems: Models and spectral efficiency performance," *IEEE Wireless Communications*, vol. 25, no. 2, pp. 24–31, Apr. 2018.
- [3] M. S. Ali, E. Hossain, A. Al-Dweik, and D. I. Kim, "Downlink power allocation for CoMP-NOMA in multi-cell networks," *IEEE Transactions on Communications*, vol. 66, no. 9, pp. 3982–3998, Sept. 2018.
- [4] Y. Tian, A. Nix, and M. Beach, "On the performance of a multi-tier NOMA strategy in coordinated multi-point networks," *IEEE Communications Letters*, vol. 21, no. 11, pp. 2448–2451, Nov. 2017.
- [5] Y. Tian, A. R. Nix, and M. Beach, "On the performance of opportunistic NOMA in downlink CoMP networks," *IEEE Communications Letters*, vol. 20, no. 5, pp. 998–1001, May 2016.
- [6] Z. Liu, G. Kang, L. Lei, N. Zhang, and S. Zhang, "Power allocation for energy efficiency maximization in downlink CoMP systems with NOMA," in *Proc. IEEE Wireless Communications and Networking Conference (WCNC)*, Mar. 2017, pp. 1–6.
- [7] I. Khan, F. Belqasmi, R. Glitho, N. Crespi, M. Morrow, and P. Polakos, "Wireless sensor network virtualization: A survey," *IEEE Communications Surveys Tutorials*, vol. 18, no. 1, pp. 553–576, Mar. 2016.
- [8] D. B. Rawat, "A novel approach for shared resource allocation with wireless network virtualization," in *Proc. IEEE International Conference on Communications Workshops (ICC Workshops)*, May 2017, pp. 665–669.
- [9] E. J. Kitindi, S. Fu, Y. Jia, A. Kabir, and Y. Wang, "Wireless network virtualization with SDN and C-RAN for 5G networks: Requirements, opportunities, and challenges," *IEEE Access*, vol. 5, pp. 19 099–19 115, Sept. 2017.
- [10] L. Li, N. Deng, W. Ren, B. Kou, W. Zhou, and S. Yu, "Multi-service resource allocation in future network with wireless virtualization," *IEEE Access*, vol. 6, pp. 53 854–53 868, Sept. 2018.
- [11] H. Weingarten, Y. Steinberg, and S. S. Shamai, "The capacity region of the gaussian multiple-input multiple-output broadcast channel," *IEEE Transactions on Information Theory*, vol. 52, no. 9, pp. 3936–3964, 2006.
- [12] W. Yu and T. Lan, "Transmitter optimization for the multi-antenna downlink with per-antenna power constraints," *IEEE Transactions on Signal Processing*, vol. 55, no. 6, pp. 2646–2660, 2007.
- [13] S. Shamai and B. M. Zaidel, "Enhancing the cellular downlink capacity via co-processing at the transmitting end," in *Proc. 53rd Vehicular Technology Conference*, vol. 3, 2001, pp. 1745–1749 vol.3.
- [14] A. E. Gamal and Y.-H. Kim, *Network Information Theory*. USA: Cambridge University Press, 2012.
- [15] M. Vaezi, Z. Ding, and H. V. Poor, *Multiple Access Techniques for 5G Wireless Networks and Beyond*, 1st ed. Springer Publishing Company, Incorporated, 2018.
- [16] M. Vaezi, R. Schober, Z. Ding, and H. V. Poor, "Non-orthogonal multiple access: Common myths and critical questions," *IEEE Wireless Communications*, vol. 26, no. 5, pp. 174–180, 2019.
- [17] W. Shin, M. Vaezi, B. Lee, D. J. Love, J. Lee, and H. V. Poor, "Non-orthogonal multiple access in multi-cell networks: Theory, performance, and practical challenges," *IEEE Communications Magazine*, vol. 55, no. 10, pp. 176–183, 2017.
- [18] X. Sun, N. Yang, S. Yan, Z. Ding, D. W. K. Ng, C. Shen, and Z. Zhong, "Joint beamforming and power allocation in downlink NOMA multiuser MIMO networks," *IEEE Transactions on Wireless Communications*, vol. 17, no. 8, pp. 5367–5381, Aug. 2018.
- [19] Y. Al-Eryani, E. Hossain, and D. I. Kim, "Generalized coordinated multipoint (GCoMP)-enabled NOMA: Outage, capacity, and power allocation," *IEEE Transactions on Communications*, vol. 67, no. 11, pp. 7923–7936, Nov. 2019.
- [20] L. Lei, D. Yuan, C. K. Ho, and S. Sun, "Power and channel allocation for non-orthogonal multiple access in 5G systems: Tractability and computation," *IEEE Transactions on Wireless Communications*, vol. 15, no. 12, pp. 8580–8594, Dec. 2016.
- [21] F. Fang, H. Zhang, J. Cheng, and V. C. M. Leung, "Energy-efficient resource allocation for downlink non-orthogonal multiple access network," *IEEE Transactions on Communications*, vol. 64, no. 9, pp. 3722–3732, Sept. 2016.
- [22] B. Di, L. Song, and Y. Li, "Sub-channel assignment, power allocation, and user scheduling for non-orthogonal multiple access networks," *IEEE Transactions on Wireless Communications*, vol. 15, no. 11, pp. 7686–7698, Nov. 2016.

- [23] Z. Ding, X. Lei, G. K. Karagiannidis, R. Schober, J. Yuan, and V. K. Bhargava, "A survey on non-orthogonal multiple access for 5G networks: Research challenges and future trends," *IEEE Journal on Selected Areas in Communications*, vol. 35, no. 10, pp. 2181–2195, 2017.
- [24] S. M. R. Islam, N. Avazov, O. A. Dobre, and K. Kwak, "Power-domain non-orthogonal multiple access (NOMA) in 5G systems: Potentials and challenges," *IEEE Communications Surveys & Tutorials*, vol. 19, no. 2, pp. 721–742, 2017.
- [25] F. Liu and M. Petrova, "Performance of dynamic power and channel allocation for downlink MC-NOMA systems," *IEEE Transactions on Wireless Communications*, vol. 19, no. 3, pp. 1650–1662, Mar. 2020.
- [26] C. Chung and C. Ku, "Selective transmission strategy for NOMA in downlink CoMP," in *Proc. IEEE 89th Vehicular Technology Conference (VTC2019-Spring)*, 2019, pp. 1–5.
- [27] A. Kilzi, J. Farah, C. Abdel Nour, and C. Douillard, "Mutual successive interference cancellation strategies in NOMA for enhancing the spectral efficiency of CoMP systems," *IEEE Transactions on Communications*, vol. 68, no. 2, pp. 1213–1226, Feb. 2020.
- [28] J. Jose, A. Ashikhmin, P. Whiting, and S. Vishwanath, "Channel estimation and linear precoding in multiuser multiple-antenna TDD systems," *IEEE Transactions on Vehicular Technology*, vol. 60, no. 5, pp. 2102–2116, June 2011.
- [29] T. A. Thomas and F. W. Vook, "Method for obtaining full channel state information for RF beamforming," in *Proc. IEEE Global Communications Conference*, Dec. 2014, pp. 3496–3500.
- [30] D. Tweed, S. Parsaefard, M. Derakhshani, and T. Le-Ngoc, "Dynamic resource allocation for MC-NOMA VWNs with imperfect SIC," in *Proc. IEEE 28th Annual International Symposium on Personal, Indoor, and Mobile Radio Communications (PIMRC)*, Oct. 2017, pp. 1–5.
- [31] T. M. Ho, N. H. Tran, S. M. A. Kazmi, Z. Han, and C. S. Hong, "Wireless network virtualization with non-orthogonal multiple access," in *Proc. NOMS 2018 - 2018 IEEE/IFIP Network Operations and Management Symposium*, Apr. 2018, pp. 1–9.
- [32] J. Choi, "Non-orthogonal multiple access in downlink coordinated two-point systems," *IEEE Communications Letters*, vol. 18, no. 2, pp. 313–316, Feb. 2014.
- [33] Z. Yang, C. Pan, W. Xu, Y. Pan, M. Chen, and M. El Kashlan, "Power control for multi-cell networks with non-orthogonal multiple access," *IEEE Transactions on Wireless Communications*, vol. 17, no. 2, pp. 927–942, Feb. 2018.
- [34] Y. Fu, Y. Chen, and C. W. Sung, "Distributed power control for the downlink of multi-cell NOMA systems," *IEEE Transactions on Wireless Communications*, vol. 16, no. 9, pp. 6207–6220, Sept. 2017.
- [35] M. Moltafet, R. Joda, N. Mokari, M. R. Sabagh, and M. Zorzi, "Joint access and fronthaul radio resource allocation in PD-NOMA-based 5G networks enabling dual connectivity and CoMP," *IEEE Transactions on Communications*, vol. 66, no. 12, pp. 6463–6477, 2018.
- [36] L. You, D. Yuan, L. Lei, S. Sun, S. Chatzinotas, and B. Ottersten, "Resource optimization with load coupling in multi-cell NOMA," *IEEE Transactions on Wireless Communications*, vol. 17, no. 7, pp. 4735–4749, 2018.
- [37] Y. Xu, C. Shen, Z. Ding, X. Sun, S. Yan, G. Zhu, and Z. Zhong, "Joint beamforming and power-splitting control in downlink cooperative SWIPT NOMA systems," *IEEE Transactions on Signal Processing*, vol. 65, no. 18, pp. 4874–4886, Sept. 2017.
- [38] Y. Sun, D. W. K. Ng, Z. Ding, and R. Schober, "Optimal joint power and subcarrier allocation for full-duplex multicarrier non-orthogonal multiple access systems," *IEEE Transactions on Communications*, vol. 65, no. 3, pp. 1077–1091, Mar. 2017.
- [39] Y. Fu, L. Salaün, C. W. Sung, and C. S. Chen, "Subcarrier and power allocation for the downlink of multicarrier NOMA systems," *IEEE Transactions on Vehicular Technology*, vol. 67, no. 12, pp. 11 833–11 847, 2018.
- [40] S. Rezvani, S. Parsaefard, N. Mokari, M. R. Javan, and H. Yanikomeroglu, "Cooperative multi-bitrate video caching and transcoding in multicarrier NOMA-assisted heterogeneous virtualized MEC networks," *IEEE Access*, vol. 7, pp. 93 511–93 536, July 2019.
- [41] S. Rezvani and E. A. Jorswieck, "Cache replacement in CoMP-based multi-cell networks with unknown content popularity," in *Proc. 24th International ITG Workshop on Smart Antennas (WSA)*, May 2020, pp. 1–6.
- [42] A. Zappone, E. Björnson, L. Sanguinetti, and E. A. Jorswieck, "Globally optimal energy-efficient power control and receiver design in wireless networks," *IEEE Transactions on Signal Processing*, vol. 65, no. 11, p. 2844–2859, June 2017.
- [43] H. Tuy, "Monotonic optimization," *SIAM Journal on Optimization*, vol. 11, no. 2, p. 464–494, 2000.
- [44] H. Tuy, F. Al-Khayyal, and P. Thach, "Monotonic optimization: Branch and cut methods," *Essays and Surveys in Global Optimization*, pp. 39–78, 2005.

- [45] J. Zhao, Y. Liu, K. K. Chai, A. Nallanathan, Y. Chen, and Z. Han, "Spectrum allocation and power control for non-orthogonal multiple access in HetNets," *IEEE Transactions on Wireless Communications*, vol. 16, no. 9, pp. 5825–5837, Sept. 2017.
- [46] D. T. Ngo, S. Khakurel, and T. Le-Ngoc, "Joint subchannel assignment and power allocation for OFDMA femtocell networks," *IEEE Transactions on Wireless Communications*, vol. 13, no. 1, pp. 342–355, Jan. 2014.
- [47] S. Boyd and L. Vandenberghe, *Convex Optimization*. Cambridge University Press, 2009.
- [48] C. Y. Wong, R. S. Cheng, K. B. Lataief, and R. D. Murch, "Multiuser OFDM with adaptive subcarrier, bit, and power allocation," *IEEE Journal on Selected Areas in Communications*, vol. 17, no. 10, pp. 1747–1758, Oct. 1999.
- [49] M. Tao, Y. C. Liang, and F. Zhang, "Resource allocation for delay differentiated traffic in multiuser OFDM systems," *IEEE Transactions on Wireless Communications*, vol. 7, no. 6, pp. 2190–2201, June 2008.